Chapter 17
CAD, A Multienzymatic Protein at the Head of de Novo Pyrimidine Biosynthesis

Francisco del Caño-Ochoa, María Moreno-Morcillo and Santiago Ramón-Maiques

Abstract CAD is a 1.5 MDa particle formed by hexameric association of a 250 kDa protein that carries the enzymatic activities for the first three steps in the de novo biosynthesis of pyrimidine nucleotides: glutamine-dependent Carbamoyl phosphate synthetase, Aspartate transcarbamoylase and Dihydroorotase. This metabolic pathway is essential for cell growth and proliferation and is conserved in all living organisms. However, the fusion of the first three enzymatic activities of the pathway into a single multienzymatic protein only occurs in animals. In prokaryotes, by contrast, these activities are encoded as distinct monofunctional enzymes that function independently or by forming more or less transient complexes. Whereas the structural information about these enzymes in bacteria is abundant, the large size and instability of CAD has only allowed a fragmented characterization of its structure. Here we retrace some of the most significant efforts to decipher the architecture of CAD and to understand its catalytic and regulatory mechanisms.

Keywords Glutaminase · Carbamoyl phosphate synthetase · Aspartate transcarbamoylase · Dihydroorotase · Nucleotide metabolism · PALA · Metabolic disease

F. del Caño-Ochoa · M. Moreno-Morcillo · S. Ramón-Maiques (✉)
Department of Genome Dynamics and Function, Centro de Biología Molecular Severo Ochoa (CSIC-UAM), Nicolas Cabrera 1, 28049 Madrid, Spain
e-mail: santiago.ramon@cbm.csic.es

F. del Caño-Ochoa
e-mail: fdelcano@cbm.csic.es

M. Moreno-Morcillo
e-mail: mmoreno@cbm.csic.es

J. R. Harris and J. Marles-Wright (eds.), *Macromolecular Protein Complexes II: Structure and Function*, Subcellular Biochemistry 93,
https://doi.org/10.1007/978-3-030-28151-9_17

The de Novo Biosynthetic Pathway for Pyrimidines

Nucleotides are essential compounds for all forms of life as building blocks for RNA and DNA synthesis. Uracil, thymine and cytosine are the three major pyrimidine bases for the formation of nucleic acids. These pyrimidines also exist as free nucleotides (e.g. uridine 5-phosphate, UMP) or nucleosides (e.g. uridine) in living tissues where they act as allosteric regulators or as coenzymes (Brown 1998). In addition, uridine diphosphate (UDP) and cytidine diphosphate (CDP) play prominent roles as activators and carriers of intermediate metabolites: UDP-glucose is required for protein glycosylation and for the biosynthesis of polysaccharides (e.g. glycogen, cellulose), and CDP-activated compounds (e.g. CDP-choline, CDP-ethanolamine) are important intermediates for the biosynthesis of phospholipids.

The cells require a constant supply of pyrimidines that can be obtained by two different pathways (Fig. 17.1). Pyrimidines can be synthetized de novo from small precursors such as ammonia, bicarbonate, ATP, aspartate (Asp) and 5-phosphoribosyl-1-pyrophosphate (PRPP) (Jones 1980). Alternatively, organisms can employ different recycling or salvage pathways to uptake preformed pyrimidine bases (uracil) or nucleosides (uridine) released during the turnover of nucleic acids or acquired from the diet (Nyhan 2005). The relative contribution of de novo and salvage pathways is dependent upon cell type and developmental stage (Evans and Guy 2004). In general, fully differentiated and quiescent cells obtain pyrimidines through salvage pathways and the de novo synthesis is low. Contrary, the de novo biosynthesis is needed to fuel the high demand of pyrimidines during cell growth and proliferation.

The metabolic pathway leading to de novo synthesis of UMP consists of six sequential enzymatic reactions that are preserved in all living organisms, from microorganisms to humans (Jones 1980). Figure 17.1 depicts this process as an assembly line, where the product of one enzyme acts as the substrate of the next, and the semi-finished intermediates move somehow between active centers. The metabolic pipeline starts with the manufacturing of carbamoyl phosphate (CP), a labile and high-energy phosphate metabolite that is also a common precursor for the de novo biosynthesis of arginine and urea (Jones 1980; Shi et al. 2018). CP is made from bicarbonate, ammonia (obtained from glutamine hydrolysis) and two molecules of ATP, in a four-step reaction catalyzed by carbamoyl phosphate synthetase (CPS; EC 6.3.5.5), an enzyme actually composed of two activities, a glutamine-dependent amidotransferase (GLN) and a synthetase (SYN) (Meister 1989; Simmer et al. 1990). In a second step, CP and Asp are used by the enzyme aspartate transcarbamoylase (ATC; EC 2.1.3.2) to form carbamoyl aspartate. Next, the enzyme dihydroorotase (DHO; EC 3.5.2.3) catalyzes the condensation of carbamoyl aspartate to dihydroorotate, the first cyclic compound of the pathway. Dihydroorotate is further oxidized to orotate by dihydroorotate dehydrogenase (DHODH; EC 1.3.5.2), an enzyme that in eukaryotes is tethered to the outer face of the inner mitochondrial membrane and couples pyrimidine synthesis to the respiratory chain (Fig. 17.1). Orotate is a completed pyrimidine base and is incorporated

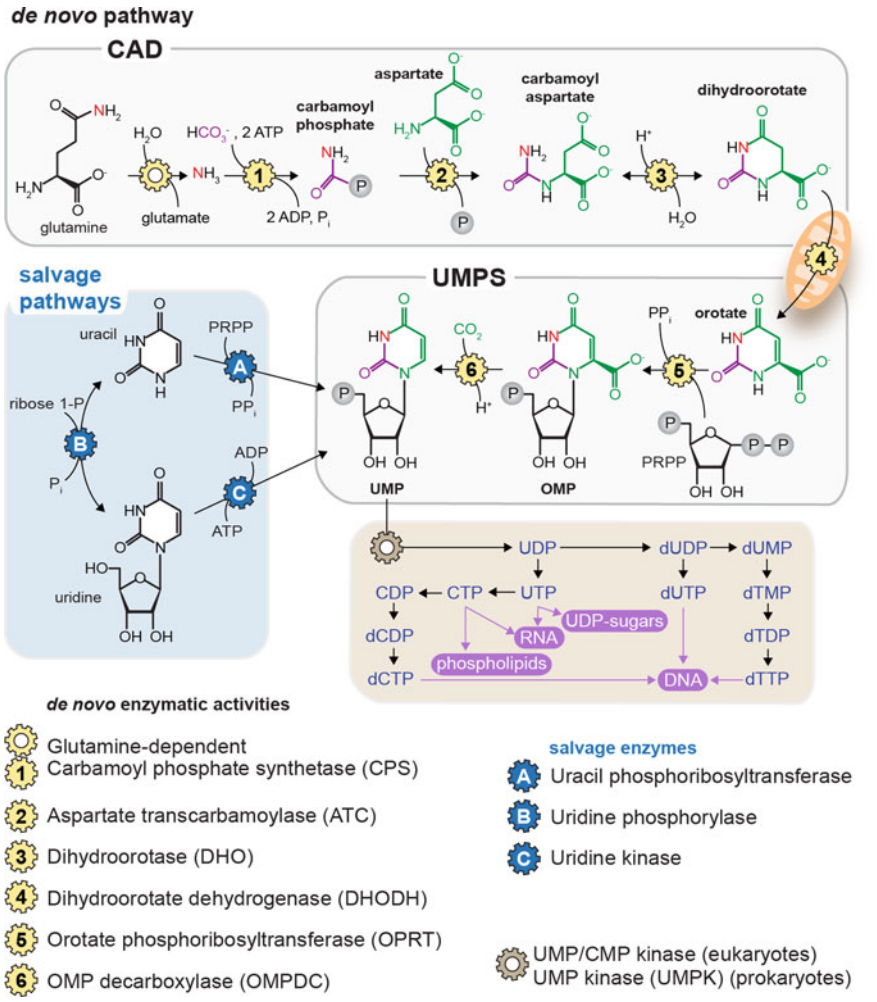

Fig. 17.1 Schematic outline of de novo and salvage pathways for pyrimidine biosynthesis in animals. The reactions catalyzed by the cytosolic multienzymatic proteins CAD and UMPS are framed in grey background, while the intermediate step occurs in the mitochondria. The salvage pathways for recycling of uracil or uridine are indicated in blue background. The numerous reactions that transform UMP into the pool of different pyrimidine nucleotides are represented in brownish background, with final fates for the different nucleotides shown in pink

to the activated sugar PRPP by the enzyme orotate phosphoribosyltransferase (OPRT; EC 2.4.2.10), producing the nucleotide orotidine 5-phosphate (OMP). Lastly, the OMP decarboxylase (OMPDC; EC 4.1.1.23) converts OMP to UMP, which is subsequently phosphorylated to UDP and UTP by different kinase activities. It is from these nucleotides that the other common pyrimidine derivatives arise (Fig. 17.1).

Although the six enzymatic steps for de novo manufacturing of UMP are evolutionary conserved, the organization of the enzymatic activities varies greatly in prokaryotes, protists, plants, fungi, and animals (Fig. 17.2a). In most prokaryotes and plants, the first three reactions are catalyzed by distinct enzymes that work independently or by forming more or less transient complexes (Jones 1980; Zrenner et al. 2006). In these organisms a single CPS, formed by association of two distinct proteins with GLN and SYN activities, makes CP both for the synthesis of pyrimidine and arginine, and thus, ATC becomes the first committed enzyme for de novo pyrimidine synthesis. In some bacteria, like *Escherichia coli*, ATC is under a strict allosteric control, being feedback inhibited by the pyrimidine nucleotides UTP and CTP and activated by a purine nucleotide, ATP [reviewed in (Allewell 1989; Jacobson and Stark 1973)]. The enzyme is formed by two trimers of catalytic subunits related by three dimers of regulatory subunits where nucleotide effectors bind, inducing large conformational changes in the holoenzyme [reviewed in (Lipscomb 1994)] (Fig. 17.2b). In other bacteria, ATC is not regulated and consists of a catalytic trimer without regulatory subunits that functions independently or forming a non-covalent complex with DHO (Fig. 17.2c).

The scenario is more puzzling in other organisms, where the enzymatic activities appear highly organized. Early studies indicated that in simple eukaryotes, such as *Neurospora* or *Saccharomyces*, two CPSs provide distinct intracellular CP pools for pyrimidine and arginine synthesis (Fig. 17.2a). The arginine-specific CPS, formed like in bacteria by the non-covalent association of two proteins with GLN and SYN activities, locates in the mitochondria (Lacroute et al. 1965), whereas the pyrimidine-specific CPS and ATC activities are present in a single bi-functional protein encoded by the genes *pyr-3* in *Neurospora* (Williams et al. 1970; Williams and Davis 1970) or *ura2* in *S. cerevisiae* (Lue and Kaplan 1969). This bi-functional protein also contains an inactive DHO-like domain, and these organisms have a monofunctional DHO enzyme encoded by an independent gene (*ura4* in *S. cerevisiae*) (Denis-Duphil 1989; Souciet et al. 1989) (Fig. 17.2a). Thus, in fungi only five genes code for the six enzymatic activities for UMP synthesis.

Similarly, in animals, distinct mitochondrial and cytosolic CPSs make CP pools for arginine and pyrimidine synthesis, respectively (Jones 1980) (Fig. 17.2a). In most terrestrial vertebrates, there is an arginine-specific CPS (CPS-1; EC. 6.3.4.16) formed by the fusion of an inactive GLN domain and a SYN domain, which is only expressed in the mitochondria of hepatocytes and requires acetylglutamate as a co-factor (Jones 1980; Rubio et al. 1981). CPS-1 cannot hydrolyze glutamine and is used to detoxify free-ammonia directly through the urea cycle. On the other hand, early studies proved the existence of a pyrimidine-specific CPS (CPS-2) that co-purified with the ATC activity in some sort of cytosolic complex (Hoogenraad et al. 1971).[1] Unlike in fungi, this complex also contained DHO activity (Shoaf and

[1]There is yet a CPS-3 in some invertebrates and fish that combines properties of CPS-1 and CPS-2 [Anderson PM (1989) Biochem J 261(2): 523–529]. It consists of a single polypeptide with GLN and SYN domains, requires acetylglutamate as co-factor, is not regulated by nucleotides and hydrolyzes glutamine.

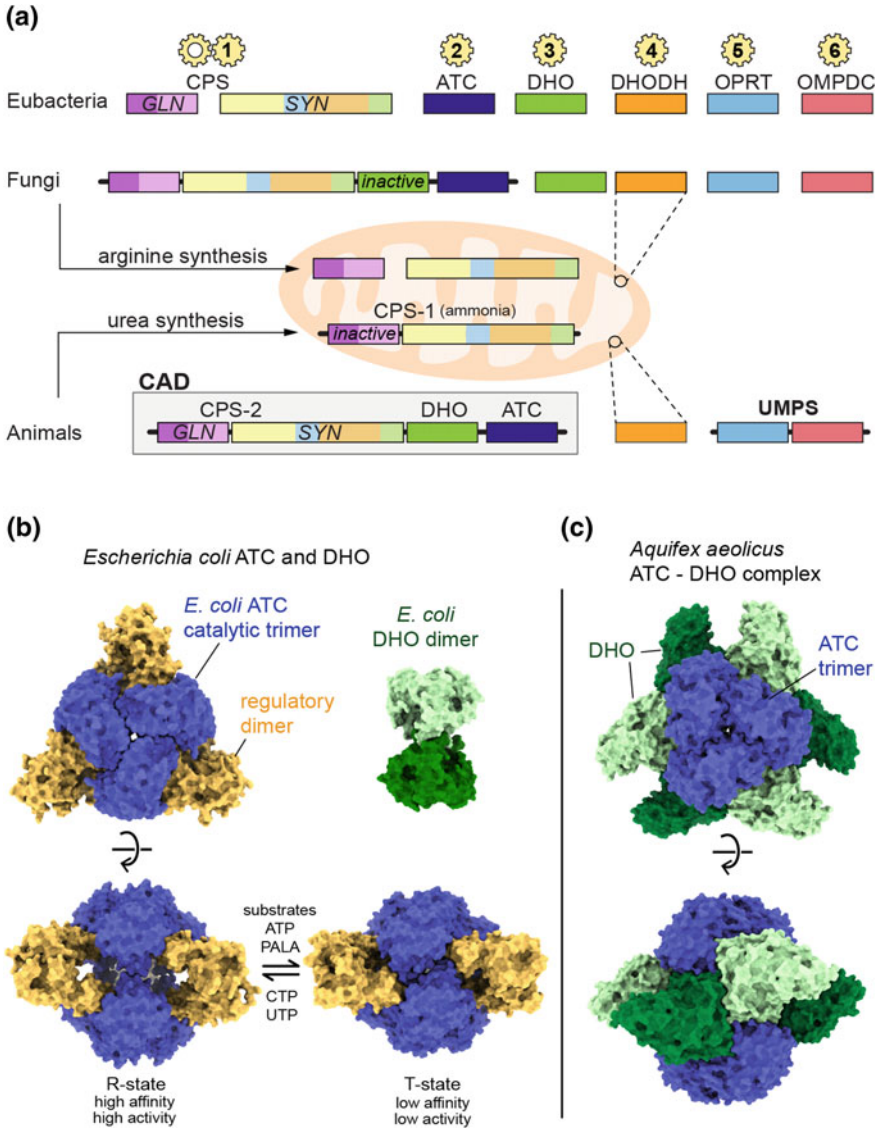

Fig. 17.2 Organization of the enzymes involved in de novo pyrimidine biosynthesis. **a** Schematic representation of the six enzymatic activities needed for de novo pyrimidine biosynthesis of UMP in eubacteria, fungi and animals. The rectangles represent individual proteins or domains within multienzymatic proteins. A second arginine-specific CPS present in the mitochondria of fungi and some animals is also shown. **b**, **c** Space filling representation of the ATC and DHO enzymes in *Escherichia coli* (**b**) and *Aquifex aeolicus* (**c**). *E. coli* ATC is an holoenzyme formed by two trimers of catalytic subunits related by three dimers of regulatory subunits. The enzyme undergoes conformational transitions between active (R) and inactive (T) states regulated by the binding of substrates, inhibitors and allosteric effectors. In *A. aeolicus*, ATC and DHO enzymes are intimately associated forming a heterododecamer

Jones 1971), leading M. E. Jones to postulate that the initial three enzymes for the de novo biosynthesis in mammals could form a stable complex or be part of a single multienzymatic protein. This association was named CAD for the first letters of the distinct enzymatic activities, and was subsequently found in every animal species investigated, from *Dictyostelium* to human [reviewed in (Evans 1986; Jones 1980)].

The nature of this multienzymatic association was not unveiled until it was purified to homogeneity by the group of G. Stark from hamster cells treated with the drug PALA (N-phosphonacetyl-L-aspartate). PALA was synthetized as a potent inhibitor of *E. coli* ATC that combines features of both enzyme substrates (CP and Asp) and was postulated to mimic the transition state of the reaction (Collins and Stark 1971). PALA was also effective in inhibiting the growth of mouse tumors, proving that de novo pyrimidine synthesis is required for cell proliferation (Swyryd et al. 1974; Yoshida et al. 1974). However, some of the cells developed resistance to the inhibitory effect of PALA by producing more than 100 times the original activity of the three-enzyme complex (Kempe et al. 1976). When the complex was isolated from these overproducing cells, the three catalytic activities were found integrated within a single polypeptide of ~250 kDa that self-associated in a mixture of oligomeric forms, mostly trimers and hexamers (Coleman et al. 1977; Kempe et al. 1976). This physical association between the three enzymes was confirmed by a combined genetic, biochemical and immunological approach using CAD defective mutants in CHO cells (Davidson and Patterson 1979).

The attempts to purify CAD revealed its extraordinary susceptibility to proteolytic cleavage, which allowed the isolation of different protein fragments retaining different enzymatic activities (Davidson et al. 1981; Evans 1986; Kim et al. 1992; Mally et al. 1981). The analysis of the proteolytic fragments and of mutants in the CAD locus in *Drosophila* (*rudimentary* gene) provided strong evidence of a simple domain structure, where enzymatic activities were present in CAD as different functional domains connected by more or less unstructured linker regions. The correct order of the domains, GLN-SYN-DHO-ATC (Fig. 17.2a), was not confirmed until the genes from different organisms were fully sequenced [*Drosophila* (Freund and Jarry 1987); hamster (Shigesada et al. 1985); human (Davidson et al. 1990); *Dictiostelyum* (Faure et al. 1989); and *S. cerevisiae ura2* (Denis-Duphil 1989; Souciet et al. 1989)].

In addition, a number of gene dissection experiments proved that fragments of CAD could complement *E. coli* deficient in CPS, DHO or ATC activities, indicating that the isolated enzymatic CAD domains were functional and topologically independent [reviewed in (Davidson et al. 1993)].

CAD is not the only multienzymatic protein in the de novo pyrimidine pathway. In animals (and also in plants), the OPRT and OMPDC activities, are also fused into a single bi-functional protein named UMP synthetase (UMPS) (Fig. 17.2a) (Jones 1980; Traut and Jones 1979). Thus, two cytosolic multienzymatic proteins are responsible for catalyzing five out of six steps in UMP synthesis in animals (Jones 1980; Shoaf and Jones 1971), while the reaction catalyzed by the dehydrogenase occurs inside the mitochondria (Fig. 17.1).

The evolutionary diversity shown in Fig. 17.2a is difficult to reconcile with the view of a metabolic assembly line formed by enzymes functioning as autonomous catalytic units. Enzymes work more efficiently when assembled into complexes that favor the communication, coordination and interdependence of the different activities and have the potential to express unique catalytic and regulatory properties (Gaertner 1978). Likely, the most effective of these interactions is the covalent linkage into a multienzymatic conjugate such as CAD. We are familiar with the dynamics that improve the relation with co-workers in our everyday life at the laboratory or in the office. Now, we want to understand whether and how enzymes apply similar teamwork strategies to make pyrimidines in the most efficient manner.

Although bacterial CPS, ATC and DHO enzymes are well characterized both structurally and biochemically, the large size of CAD and the high sensitivity to proteases hampered many structural characterization attempts so far. In this chapter, we retrace some of the most significant efforts to decipher the structure of CAD and to understand its functioning.

Starting from the Beginning: The GLN and SYN Domains

CP is a small and highly unstable molecule that requires a truly remarkable protein machinery of more than one thousand aminoacids for its synthesis. The reaction involves three discrete chemical steps with canalization of highly reactive and unstable intermediates: carboxyphosphate, ammonia and carbamate (Anderson and Meister 1965; Meister 1989) (Fig. 17.3a). In a first step, a molecule of bicarbonate is phosphorylated at the expense of one ATP molecule to form carboxyphosphate and ADP. Then, a molecule of ammonia obtained directly (urea cycle CPS-1) or hydrolyzed from glutamine reacts with the carboxyphosphate to form carbamate and inorganic phosphate. In a final step, carbamate is phosphorylated by consuming a second ATP molecule to form CP.

All known CPSs share a common reaction mechanism, and present substantial sequence homology and similar multidomain architecture. As previously mentioned, CPS is composed of two parts, a $\sim$40 kDa GLN that delivers ammonia and a $\sim$120 kDa SYN that catalyzes the three-step reaction mentioned above. The GLN and SYN parts exist either as different subunits, such as in bacterial CPSs or in the arginine-specific CPS in fungi, or they are connected by a short linker within a single polypeptide, such as in the urea-cycle CPS-1 (Fig. 17.2a). Alternatively, GLN and SYN can be fused together with ATC and DHO (or an inactive DHO-like domain) forming the CAD (or CAD-like) multienzymatic protein. Currently, only the structures of the CPS from *E. coli* and the ammonia-dependent CPS-1 from human hepatocytes have been characterized.

E. coli CPS has been extensively studied both biochemically and structurally (Holden et al. 1998; Meister 1989; Raushel et al. 1998; Thoden et al. 1998, 1999a, b, c, d, 2002, 2004). The enzyme is a stable heterodimer formed by the small GLN

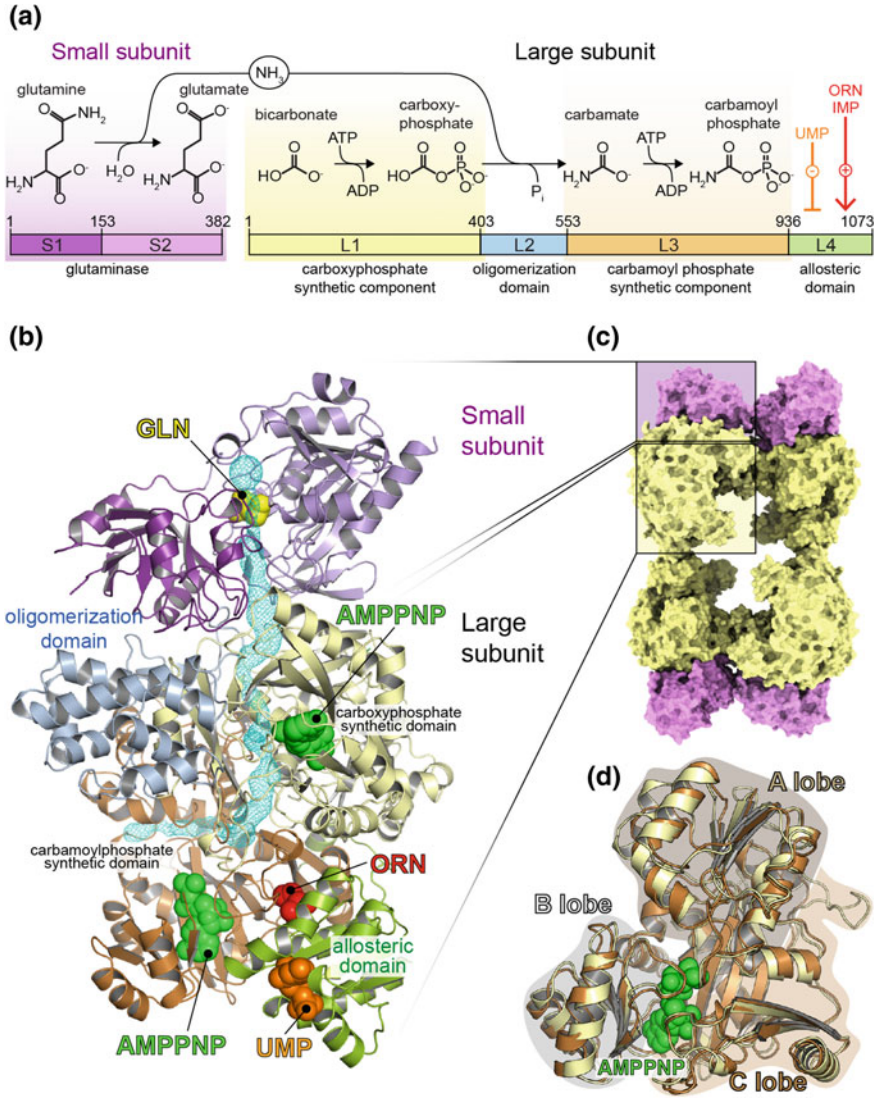

Fig. 17.3 *E. coli* CPS structure. **a** Schematic representation of the small and large subunits of *E. coli* CPS and partial reactions catalyzed by each domain within the protein. The binding of allosteric effectors to the C-terminal region of the protein is indicated. **b** Cartoon representation of the enzyme heterodimer, with domains colored as in (**a**). Glutamine (GLN), AMPPNP (a non-hydrolyzable analog of ATP), UMP and ornithine (ORN) are represented as spheres. The internal tunnel connecting the three active sites is represented as cyan mesh. **c** Space filling representation of *E. coli* CPS tetramer as found in the crystal structure. **d** Superposition of the carboxyphosphate synthetic component (L1; shown in yellow) and the carbamoyl phosphate synthetic component (L3; orange) with AMPPNP represented as spheres. The A, B and C lobes forming the ATP-grasp fold are indicated

subunit and the large SYN subunit (Fig. 17.3a), encoded respectively by the genes *carA* and *carB*. The large subunit, also holds the binding sites for the allosteric regulators. Although the GLN/SYN heterodimer is the functional unit of *E. coli* CPS, the protein readily converts to a dimer or a tetramer with unaffected catalytic properties (Anderson 1986) (Fig. 17.3c).

CPS-1, on the other hand, is a protein of 1500 amino acids divided into an inactive N-terminal GLN domain and a C-terminal SYN domain, which correspond respectively, to the small and large subunits of bacterial CPS (Fig. 17.4a). The structure of human CPS-1 probed to be highly similar to that of *E. coli* CPS (de Cima et al. 2015), as correctly inferred from biochemical studies (Nyunoya et al. 1985; Powers-Lee and Corina 1986). Despite being inactive, the GLN domain is an integral part of the enzyme and is tightly associated with the SYN domain.

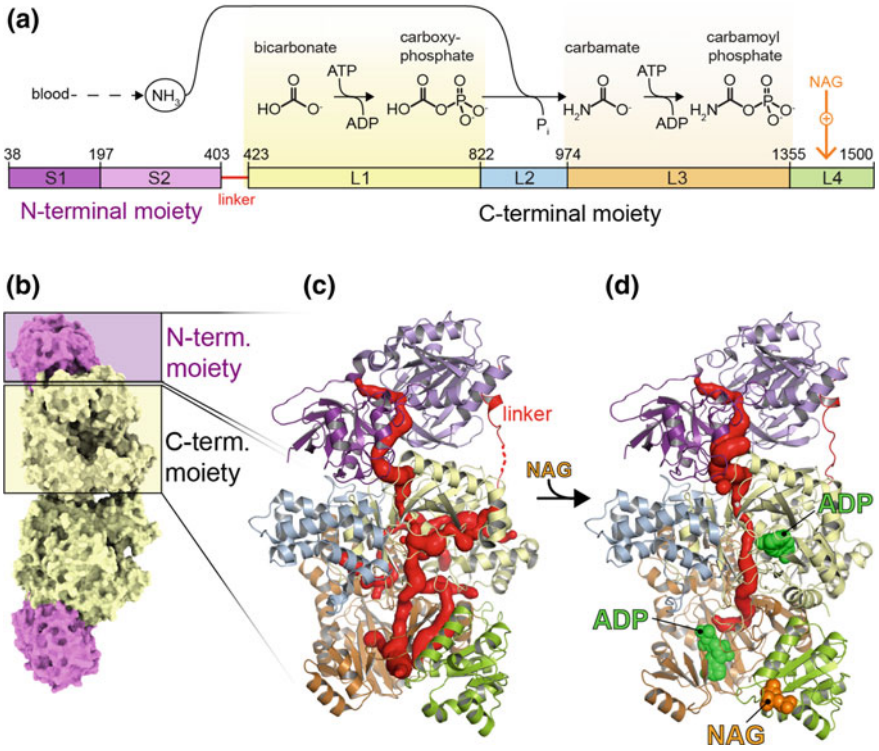

Fig. 17.4 Human CPS-1 structure. **a** Schematic representation of the enzyme with the partial reactions catalyzed by each protein region. The allosteric activation by binding of acetylglutamate (NAG) to the C-terminal region is indicated. **b** Space filling representation of CPS-1 dimer as seen in the asymmetric unit of the crystal. **c**, **d** Cartoon representation of human CPS-1 free (**c**) or bound (**d**) to NAG. Binding of NAG induces conformational changes that define the path of the tunnel - shown in red surface- through the active sites. The N- and C-terminal moieties of the protein are connected by a 20 aa linker that spans 50 Å and appears partially disordered in the structure free of acetylglutamate (indicated by a dashed line)

In solution, CPS-1 exists in a monomer-dimer rapid equilibrium where the monomer predominates (Diez-Fernandez et al. 2013; Pierson and Brien 1980; Rubio et al. 1981) (Fig. 17.4b). Both the monomers and dimers are active upon acetylglutamate binding (Lusty 1981), and there is no evidence of formation of tetramers.

So far, there is no direct structural information about the GLN or SYN domains of CAD. The CPS-2 activity of CAD is of outmost importance since it is the rate-limiting reaction in the biosynthesis of pyrimidines and the point for allosteric control (Coleman et al. 1977; Mori and Tatibana 1978). The difficulty to produce a stable construct for these regions of the protein has precluded many crystallization attempts so far. Nevertheless, the CPS-2 activity of CAD is expected to share similar structural features with *E. coli* CPS and with human CPS-1. The comparison between the structures of these evolutionary distant enzymes should give us some hints on the structure and functioning of CAD.

GLN Domain

The small subunit of *E. coli* CPS and the N-terminal moiety of human CPS-1 exhibit a globular shape divided into two lobes (Figs. 17.3 and 17.4). The N-terminal lobe of ~16 kDa (named S1) is formed by four major α-helices and two perpendicular four stranded β-sheets. The C-terminal lobe of ~25 kDa (S2) presents a central β-sheet of ten elements flanked on both sides by six α-helices, which is characteristic of the class I family of amidotransferases (Nyunoya and Lusty 1984). These glutaminases share a common reaction mechanism that involves the formation of a glutamyl-thioester intermediate between glutamine and a catalytic Cys. A conserved His is also important to activate the Cys for nucleophilic attack. In *E. coli* CPS, the catalytic residues, C269 and H353, locate at the S2 lobe, and the active site is formed at the interface with the S1 lobe (Figs. 17.3b and 17.5a). The reaction process has been delineated by different crystal structures of *E. coli* CPS bound to various ligands and bearing different mutations (Thoden et al. 1997, 1998, 1999a, c, d, 2002, 2004), and the formation of the glutamyl-thioester intermediate has been demonstrated biochemically both for *E. coli* CPS and for CAD (Chaparian and Evans 1991; Wellner et al. 1973). In contrast, human CPS-1 presents a Ser residue (S294) replacing the catalytic Cys (Fig. 17.5a), explaining why this domain is inactive.

The GLN domain of CAD is expected to be structurally similar to the GLN moieties of *E. coli* CPS and CPS-1. Sequence alignment shows the preservation of the secondary structural elements throughout the predicted S1 and S2 lobes and the conservation of active site residues, including the catalytic Cys and His residues (C252 and H336 in human CAD) (Figs. 17.5a and 17.6). Interestingly, the isolated GLN domain of hamster CAD has been produced recombinantly in bacteria but is only active when mixed in stoichiometric amounts with the large subunit of *E. coli* CPS, supporting a high degree of conservation between both enzymes (Guy and Evans 1994). It is expected that, similarly to *E. coli* CPS and human CPS-1, both

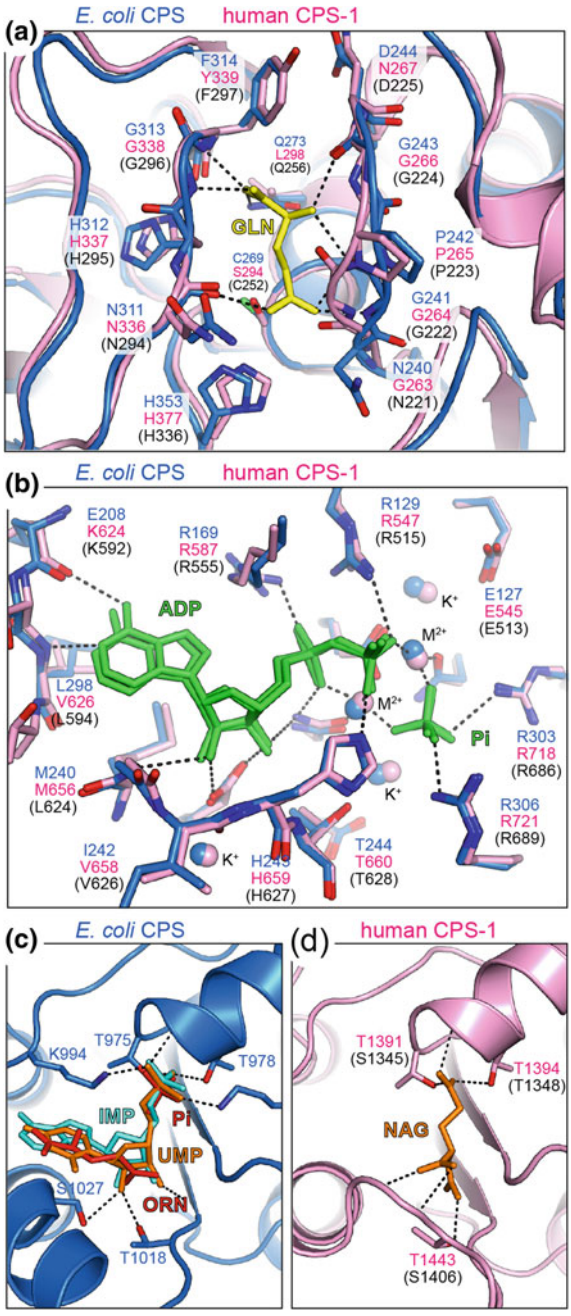

Fig. 17.5 Structural conservation between CPSs. **a** Cartoon representation of the superposition of the active site of *E. coli* CPS small subunit (blue) with the equivalent region in human CPS-1 (pink). A molecule of glutamine (GLN) bound to the *E. coli* enzyme is shown in yellow sticks and the interactions with conserved residues are indicated by dashed lines. **b** Similar representation for the superposition of the active sites of the carboxyphosphate synthetic component of *E. coli* and human CPSs. A molecule of ADP and an inorganic phosphate present in both structures are shown as green sticks. Potassium and divalent metal ions (Mg^{2+} in human CPS-1 or Mn^{2+} in *E. coli* CPS) are shown as spheres. **c** Allosteric domain of *E. coli* CPS showing the overlapping binding sites for UMP and IMP. At high concentrations, ornithine (ORN) and a molecule of inorganic phosphate (Pi) can also bind at this position. **d** Allosteric domain in human CPS-1 with acetylglutamate. In **a**, **b** and **d**, the numbers of the conserved residues in human CAD are indicated in parentheses

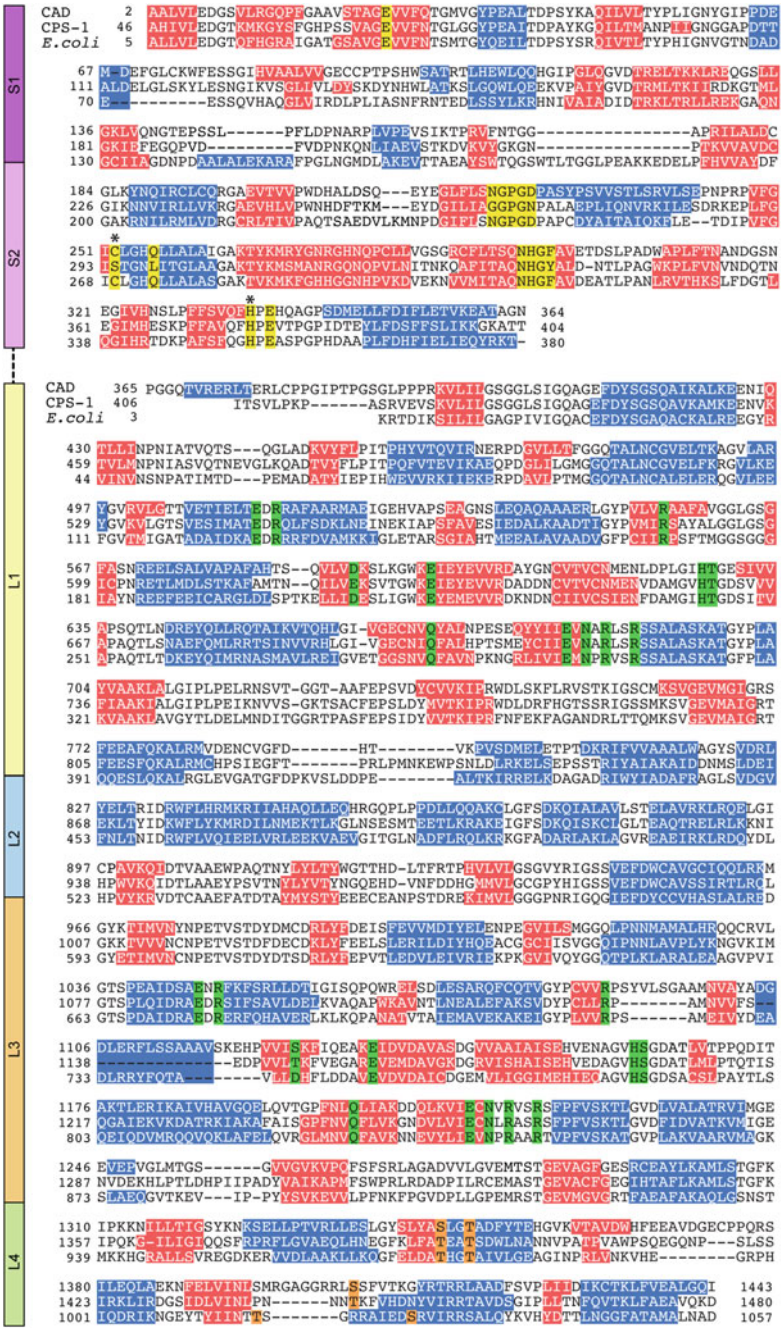
S1
S2
L1
L2
L3
L4
CAD
CPS-1
E.coli

◂**Fig. 17.6** Sequence alignments. Multiple alignment of the CPS-2 in human CAD, human CPS-1 and *E. coli* CPS sequences. A schematic diagram of the protein domains is shown on the left side. The red or blue backgrounds indicate respectively the α-helices and β-strands observed in the crystal structures or predicted from the CAD sequence. Residues involved in binding of glutamine, in the L1 or L3 phosphorylation sites and in the binding of allosteric effectors are highlighted in yellow, green and orange background, respectively. The N-terminal end of human CPS-1 corresponds to a mitochondrial targeting peptide that is cleaved off from the mature protein and is not included in the alignment

the S1 and S2 participate in an extensive interaction with the SYN domain in CAD (Figs. 17.3b and 17.4c). This interaction, which stabilizes both subunits in *E. coli* CPS (Cervera et al. 1993), somehow ensures the synchronization and enhancement of the GLN and SYN activities both in *E. coli* CPS and in CAD, likely to avoid wasteful hydrolysis of glutamine or ATP if the other substrates of the reaction are not available (Hewagama et al. 1999; Miles et al. 1998; Miles and Raushel 2000; Miran et al. 1991).

SYN Domain

The large subunit of *E. coli* CPS and the C-terminal moiety of CPS-1 are divided into four structural units (L1–4; Figs. 17.3a and 17.4a). L1 and L3 correspond to two homologous phosphorylation domains (Britton et al. 1979) that share 40% sequence identity and probably arose by a gene duplication and fusion event (Nyunoya and Lusty 1983). These two synthetic components form a pseudo-homodimer with nearly exact twofold rotational symmetry and are topologically equivalent but not identical, as expected based on their different substrates and interactions with the rest of the protein (Figs. 17.3b, d and 17.4c) (Thoden et al. 1997). L1 is the carboxyphosphate synthetic component responsible for the phosphorylation of bicarbonate and is in contact with the GLN domain. L3 is the CP component that phosphorylates carbamate and interacts with the allosteric region (L4) described below. Both synthetic components are structured in an "ATP-grasp" fold, with three lobes surrounding ("grasping") the nucleotide (Fawaz et al. 2011) (Fig. 17.3d). The A lobe (*E. coli* CPS L1 residues 1–140 and L3 residues 554–686) exhibits a modified Rossmann-fold with a five stranded β-sheet flanked on both sides by α-helices. The B lobe (*E. coli* CPS L1 residues 141–210 and L3 residues 687–756) folds in a four-stranded antiparallel β-sheet flanked on the solvent side by two α-helices. The C lobe (*E. coli* L1 residues 211–403 and L3 residues 757–936) is nucleated by an antiparallel β-sheet flanked by four helical regions. The active site, located between the B- and C-lobes, is highly similar in *E. coli* CPS and human CPS-1 (Fig. 17.5b). The nucleotide, interacting residues and divalent cations occupy virtually identical positions in both enzymes. Even the potassium ions, which are known to be required for the activity (Anderson and Meister 1966) occupy similar positions at the active sites.

The synthetic L1 and L3 domains are linked by the L2 domain, composed of seven α-helices and a two stranded β-sheet. In *E. coli* CPS, L2 participates in the formation of the tetramers, and thus it was named as the oligomerization domain (Thoden et al. 1997) (Fig. 17.3b, c). The interaction between two oligomerization domains is relatively small, as expected from the readily conversion between monomer and tetramer (Anderson 1986). In CPS-1, L2 is not involved in oligomerization and received the name of the integrating domain, for its role in embracing L1 and connecting the L1 and L3 with the GLN moiety (Fig. 17.4) (de Cima et al. 2015).

Based on the alignment of Fig. 17.6, the predicted synthetic L1 and L3 domains and the connecting L2 domain of CAD are expected to be highly similar to *E. coli* CPS and CPS-1, including the conserved catalytic residues at the phosphorylation sites (Figs. 17.5b and 17.6).

Allosteric Regulation

Most CPSs are under a strict allosteric control. Pyrimidine-specific CPSs are generally activated by the purine nucleotide inosine 5′-monophosphate (IMP) or by PRPP, a substrate for both purine and pyrimidine synthesis, and are feedback inhibited by UMP or UTP, the products of de novo pyrimidine synthesis (Jones 1980), whereas arginine-specific CPSs are generally activated by ornithine, a substrate with CP for the synthesis of arginine. CPS-1, on the other hand, is essentially an inactive enzyme that requires the activation by the co-factor acetylglutamate (Rubio et al. 1983).

E. coli CPS makes CP both for the synthesis of arginine and pyrimidines, and thus, it is inhibited by UMP and is activated by IMP and ornithine (Fig. 17.3a) (Meister 1989). These allosteric effectors regulate the activity primarily by raising or lowering the K_M for ATP nearly 10-fold (Braxton et al. 1992, 1996). Biochemical and structural studies have proven that UMP, IMP and ornithine bind at the ∼20 kDa C-terminal region of the large subunit, the L4 domain (Fig. 17.3a) (Cervera et al. 1996; Czerwinski et al. 1995; Rubio et al. 1991; Thoden et al. 1999c). This allosteric domain is structured in a Rossmann-fold (nearly identical to the A lobe in the L1 and L3 synthetic components) with a five-stranded parallel β-sheet flanked on either side by α-helices (Fig. 17.3b). UMP and IMP compete for binding in a nearly identical position at the carboxy-edge of the central β-sheet (Fig. 17.5c) (Bueso et al. 1999; Cervera et al. 1996; Mora et al. 1999; Thoden et al. 2004; Thoden et al. 1999c). Ornithine on the other hand, binds in a different pocket, 12 Å apart from the nucleotide binding site, at the interface between the allosteric domain and the CP synthetic domain (Fig. 17.3b) (Thoden et al. 1997). Some crystal structures show a second molecule of ornithine (and a phosphate ion) at the UMP/IMP binding site, likely due to the high concentrations of these ligands used in the crystallization solution (Fig. 17.5c).

Acetylglutamate also binds to the L4 domain of CPS-1 (Figs. 17.4d and 17.5d) (de Cima et al. 2015; Rodriguez-Aparicio et al. 1989). Despite having very different effector molecules, the CPS-1 and *E. coli* CPS allosteric domains are structurally very similar. Indeed, acetylglutamate occupies the equivalent position of UMP/IMP in *E. coli* CPS, and interacts with similar conserved elements (Fig. 17.5c, d).

The CPS-2 activity of CAD is allosterically inhibited by UTP and activated by PRPP, which alter the apparent K_M for ATP (Mori and Tatibana 1978). The binding of the allosteric effectors is also expected to occur at a regulatory domain at the C-terminal region of the SYN domain. This is supported by analogy to other CPSs (Rubio 1994) and because the UTP inhibition is lost when this region is deleted (Liu et al. 1994). Furthermore, E. Carrey discovered that the UTP inhibition is abolished upon phosphorylation by cAMP-dependent protein kinase A (PKA) of residue S1406 at the predicted allosteric domain (Carrey et al. 1985; Carrey and Hardie 1988). Based on sequence conservation and preservation of secondary structural elements, it is likely that the L4 domain of CPS-2 will exhibit the fold observed in *E. coli* CPS and human CPS-1. We propose that residue S1406 will occupy the equivalent position of T1443 in CPS-1, which directly binds to acetylglutamate (Figs. 17.5d and 17.6). Thus, it is feasible that a phosphorylation at residue S1406 in CAD would pose a steric impediment for the binding of UTP, as originally postulated by Carrey (Carrey 1995a).

CAD is also phosphorylated at residue T456 within the L1 domain via the MAP kinase (Erk1/2) signaling cascade (Graves et al. 2000). This modification converts UTP from an inhibitor to a modest activator and stimulates the activation by PRPP. The expected similarity with other CPSs suggests that this residue is far from the allosteric domain and thus, it is difficult to adventure a possible mechanism that explains the effect of the modification on the binding of the allosteric effectors or in the modulation of the activity.

So far, we focused the attention on CAD and ignore the comparison with the CAD-like protein from fungi. Although not shown in the alignment of Fig. 17.6, the GLN and SYN domains of CAD-like proteins are predicted to share the overall structure with other CPSs. In particular, *S. cerevisiae* URA2 has a unique binding site for UTP, likely localized at the putative L4 allosteric domain, which regulates both CPS and ATC activities (Antonelli et al. 1998), and at least in vitro, does not appear to be phosphorylated by PKA (Denis-Duphil et al. 1990). Thus, the regulatory domain appears to be conserved in all CPSs, including some that do not respond to allosteric effectors. Indeed, the unregulated arginine-specific CPS in *S. cerevisiae* (Fig. 17.2a) holds a latent allosteric domain that binds UMP and IMP, although the nucleotides do not seem to have any effect on the activity of the protein (Eroglu and Powers-Lee 2002).

A Reaction Tunnel

The *E. coli* CPS structure revealed an exceptional feature: the GLN active site is 45 Å away from the bicarbonate phosphorylation site, and this one is 35 Å apart from the phosphorylation site for carbamate (Thoden et al. 1997). Thus, the unstable reaction intermediates must be shuttled between the active centers without exposure to the bulk solvent. In *E. coli* CPS, a narrow tunnel, more than 90 Å long, runs through the interior of the protein, connecting all three active sites (Fig. 17.3b). The extensive interaction between the small subunit and the first half of the large subunit provide a safe pathway for the delivery of ammonia to the L1 active site where it will react with carboxyphosphate to form carbamate. This "ammonia" tunnel is lined by non-reactive residues that can form H-bonds with ammonia. The second portion of the tunnel transports carbamate from the L1 to the L3 active sites where it is phosphorylated to CP. This "carbamate" tunnel passes across the twofold rotational axis between the two synthetic domains and is delimited by few charged side chains to prevent the reaction with carbamate.

In human CPS-1, many of the residues that in *E. coli* CPS line the ammonia channel are conserved, but the Gly at the exit of the channel at the interface between the GLN and SYN domains is replaced by a Gln (Q318) that blocks the path (de Cima et al. 2015). This blockage explains why some CPS-1 enzymes have a complete GLN active site (e.g. CPS-1 from *Rana catesbiana*), including the catalytic Cys and His residues, but are still unable to deliver the ammonia hydrolyzed from glutamine to the SYN domain (Saeed-Kothe and Powers-Lee 2003) (de Cima et al. 2015). Likely in CPS-1, ammonia intake follows a different path to that delineated in *E. coli* CPS. It has been proposed that this alternative entry could also exist in other CPSs, including CAD, since they are active with external ammonia although at high concentrations (de Cima et al. 2015).

In *E. coli* CPS, the intramolecular tunnel is formed even in the absence of a full set of substrates. This could be due to the fact that the protein is always crystallized in presence of the allosteric activator, ornithine. In turn, the structures of human CPS-1 free or bound to acetylglutamate show important differences in the tunnel that explain in part the mechanism of activation by the co-factor (Fig. 17.4c, d). Binding of acetylglutamate causes small changes in the allosteric domain that are propagated to the L3 domain through the movement of a potassium binding loop also present in *E. coli* CPS (de Cima et al. 2015). This movement induces long-range conformational changes that stabilize the two phosphorylation sites and promote the correct formation of the reaction tunnel (de Cima et al. 2015). Similar changes triggered by the allosteric effectors are expected to occur both in *E. coli* CPS and in the SYN domain of CAD.

A Cooperative ATC Domain

The arrangement of the domains along the CAD polypeptide does not follow the order of the reactions in de novo pathway (Fig. 17.2a). The ATC domain, located at the C-end of the protein, catalyzes the second step after CPS, the transfer of the carbamoyl group of CP to the α-amino group of aspartate (Asp) to form carbamoyl aspartate (Figs. 17.1 and 17.2a) (Jones 1980).

ATC is likely one of best characterized enzymes ever. In particular, the amount of biochemical and structural information obtained on *E. coli* ATC is impressive, becoming a text-book enzyme and, together with hemoglobin, a paradigm of protein cooperativity and allosteric regulation [reviewed in (Allewell 1989; Jacobson and Stark 1973; Lipscomb 1994)]. *E. coli* ATC consists of twelve polypeptides chains: six catalytic chains of 33 kDa organized as two catalytic trimers, and six regulatory chains of 17 kDa forming three regulatory dimers (Fig. 17.2b). The affinity for the substrates is regulated both by the binding of substrates to other active sites (homotropic effects) and by the binding of nucleotide effectors to the regulatory subunits (heterotropic effects). This regulation requires the communication of conformational changes between chains and subunits (Schachman 1988). Indeed, the dissociation of the holoenzyme results in isolated catalytic trimers that are more active but lack cooperativity and allosteric regulation (Gerhart and Holoubek 1967). Numerous crystal structures of *E. coli* ATC, including the active (R) and inactive (T) states of the holoenzyme (Fig. 17.2b), and the unregulated catalytic trimer, helped to unveil the complexity of the catalytic and regulatory mechanisms (Lipscomb and Kantrowitz 2011). There are also crystal structures for other forms of ATC found in bacteria, such as the non-regulated catalytic trimers of *Bacillus subtilis* or the DHO-associated ATC from *Aquifex aeolicus* (Fig. 17.2c) (Stevens et al. 1991; Zhang et al. 2009). However, until recently, there were no structures of any eukaryotic ATC.

The ATC domain of human CAD was the first eukaryotic ATC to be structurally characterized (Ruiz-Ramos et al. 2013, 2016). As predicted (Scully and Evans 1991), the domain shows high similarity with the catalytic subunits of bacterial ATCs. The enzyme is a homotrimer with equilateral triangular appearance, and three active sites located in between subunits (Fig. 17.7a). Each subunit is divided in an N-terminal domain and a C-terminal domain of similar size, both structured by a central β-sheet of five parallel strands flanked by α-helices (Fig. 17.7b). The active site locates at the cleft between the N- and C-domains with participation of a loop (CP-loop) from the adjacent subunit. The N-terminal domain provides most of the contacts with the other subunits and holds the binding site for CP, whereas the C-domain occupies an external position at the trimer and provides the binding site for Asp. There are two mobile loops, the CP-loop at the N-domain (named loop 80s in *E. coli* ATC) and the Asp-loop at the C-domain (loop 200s in *E. coli* ATC) that appear flexibly disordered in the absence of substrates (Fig. 17.7b).

ATC catalyzes an ordered reaction, with CP binding before Asp, and carbamoyl aspartate leaving before phosphate (Collins and Stark 1969; Porter et al. 1969). CP

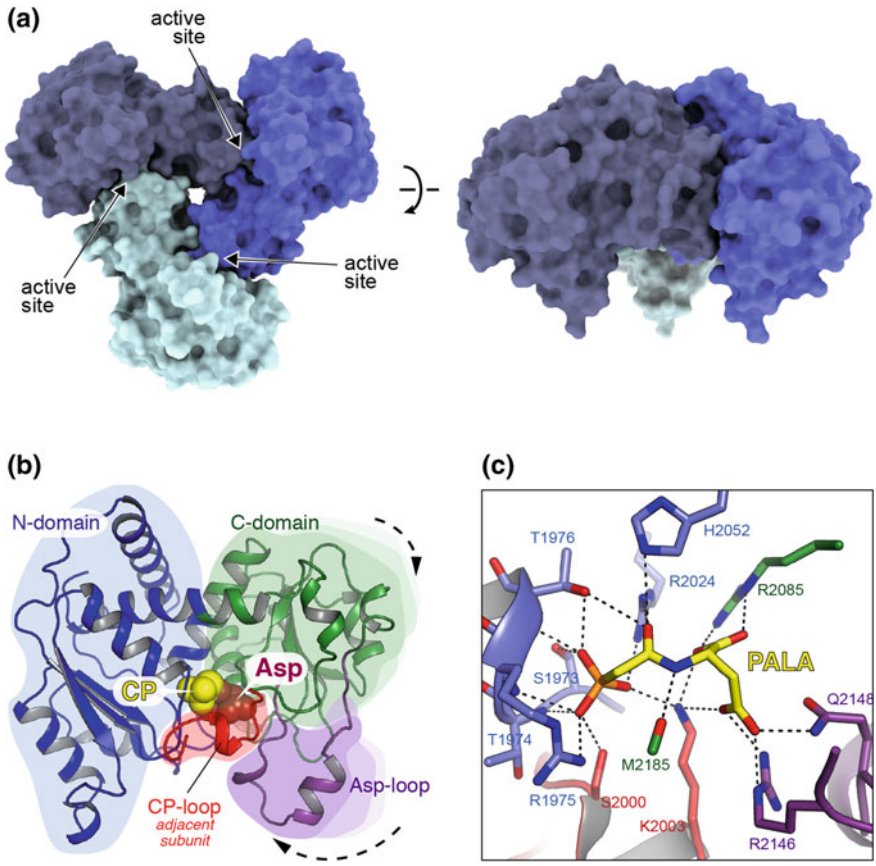

Fig. 17.7 ATC domain of human CAD. **a** Space filling representation of the trimer formed by the isolated ATC domain of human CAD in two perpendicular orientations. Each subunit is represented in a different color. **b** Cartoon representation of human ATC subunit, with the N- and C-domains represented in blue and green, respectively, and the Asp-loop depicted in purple. The arrows indicate the closure movement of the subunit upon PALA binding. PALA is shown in spheres, with the CP and the Asp moieties colored in yellow and red, respectively. The CP-loop from the adjacent subunit is depicted in red. **c** Detail of the interactions between PALA and residues at the active site

binding at the N-domain induces the positioning of the CP-loop from the adjacent subunit at the active site, and promotes a partial hinge-closure of the C-domain. These conformational changes favor the binding of Asp to a contiguous pocket in the active site. Binding of both substrates induces a further approximation between the N- and C-domains and a rigid body rotation of the Asp-loop that closes the active site (Fig. 17.7b). Overall, these movements are proposed to compress the substrates and favor the reaction (Collins and Stark 1969; Ruiz-Ramos et al. 2016).

The active sites of human and *E. coli* ATCs are indistinguishable, confirming a common reaction mechanism for both enzymes (Collins and Stark 1969; Gouaux et al. 1987; Ruiz-Ramos et al. 2016). Catalysis occurs by nucleophilic attack of the amino nitrogen of Asp on the amide carbon of CP. The phosphate group of CP or the side chain of residue H2052 (H134 in *E. coli* ATC) are likely candidates to act as general base, deprotonating and increasing the nucleophilicity of the α-amino group of aspartate, whereas the positive dipole of the nearby α-helix and the side chains of residues R2024 (R105) and H2052 (H134) act in concert to polarize the carbonyl group of CP and to stabilize the transition state of the reaction (Fig. 17.7c).

Figure 17.7c shows how every polar atom of PALA interacts with the protein, explaining the nanomolar affinity for the inhibitor (Newell et al. 1989; Ruiz-Ramos et al. 2016). The dissociation of PALA from this highly stable complex is impossible without reversing all the conformational changes, and this is a slow process that explains why the molecule acts as a nearly irreversible inhibitor. An unexpected fact is that PALA binds to human ATC with negative cooperativity: the binding of PALA to one subunit decreases the affinity for the inhibitor in the other active sites (Ruiz-Ramos et al. 2016). Indeed, only two subunits of human ATC show high affinity for PALA, while affinity for the third site is 100-fold lower. This difference with the *E. coli* ATC catalytic trimer, is likely due to a communication of conformational changes between the subunits in the human enzyme. Since PALA is proposed to resemble the transition state of the reaction, the negative cooperativity effect also suggests that in CAD, the ATC trimer might work more efficiently with only two active sites catalyzing the reaction at a time. Indeed, at high substrate concentrations, the activity of ATC is partially inhibited, suggesting that a trimer with the three subunits forced to work simultaneously might present additional intersubunit interactions that slow down the conformational movements required for catalysis (LiCata and Allewell 1997; Ruiz-Ramos et al. 2016).

In CAD, ATC catalyzes the reaction ~50-fold faster than CPS, and it has a low K_M for CP (Coleman et al. 1977; Qiu and Davidson 2000). This should facilitate that as soon as the unstable CP molecule is delivered by CPS, it will be trapped and converted by ATC. A possible asymmetry in the functioning of ATC is interesting to envision the performance of the overall activity of CAD. Perhaps the ATC subunits are fired one at a time, in some sequential process coordinated with CPS.

A DHO Domain in the Midst of CAD

DHO is a ubiquitous Zn metalloenzyme catalyzing the reversible interconversion of carbamoyl aspartate to dihydroorotate –the precursor of the pyrimidine ring– in the third step of the de novo pyrimidine biosynthesis (Fig. 17.1). Despite full conservation of the reaction, this enzyme adopts an intriguing number of different forms (Fields et al. 1999; Grande-Garcia et al. 2014). DHOs can be monomeric or dimeric proteins that function independently (e.g. *E. coli* DHO) or in association with ATC

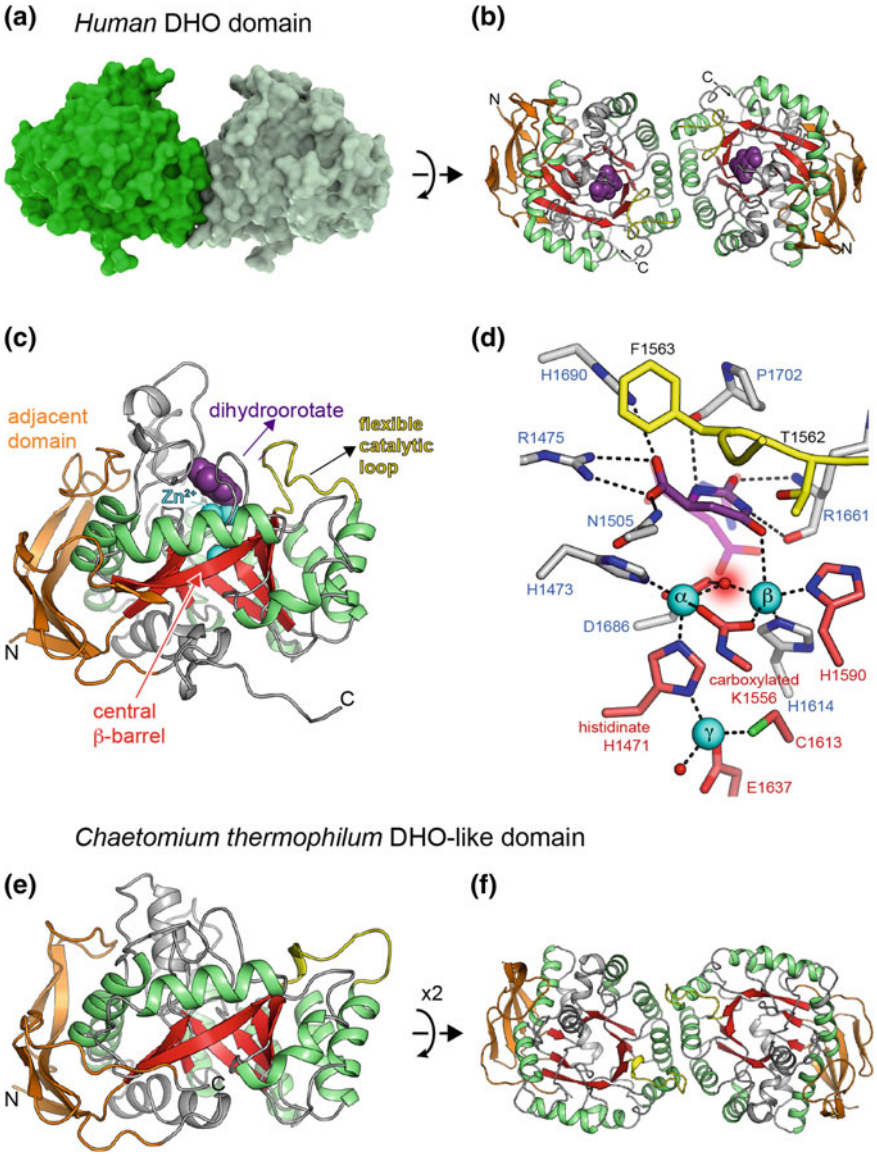

(e.g. *A. aeolicus* DHO) (Fig. 17.2b, c), or alternatively, DHO can be fused as a functional domain within CAD (Fig. 17.2a). Moreover, some DHOs seem to play a non-enzymatic role, such as the inactive DHO-like domain linking the CPS and ATC activities in the fungal CAD-like proteins (Fig. 17.2a) (Souciet et al. 1989), or the inactive DHOs that in some bacteria (e.g. *Pseudomonas aeruginosa*) form non-covalent complexes with ATC (Schurr et al. 1995). Thus, besides the well-characterized enzymatic function, DHOs seem to perform other less understood functions in the midst of the pyrimidine enzymatic machinery.

◂**Fig. 17.8** DHO domain of human CAD. **a** Space filling representation of the dimer formed by the isolated DHO domain of human CAD. **b** Cartoon view of the dimer with two molecules of dihydroorotate bound at the active sites. **c** Representation of the DHO subunit with Zn^{2+} ions and a dihydroorotate molecule represented as cyan and purples spheres, respectively. **d** Detail of the active site with dihydroorotate bound. A molecule of carbamoyl aspartate is shown in semi-transparent to show that the β-carboxylate occupies the position of the bridging water. Residues from the central β-barrel and from the loops above the barrel are colored with carbons in red and grey, respectively. The flexible loop is depicted in yellow. **e** Cartoon representation of *C. thermophilum* inactive DHO-like subunit (**e**) and dimer (**f**). The orientations and colors are as in (**b**) and (**c**) to highlight similarities with human DHO

Although the crystal structures of different bacterial DHOs were known (Fig. 17.2b, c) (Thoden et al. 2001; Zhang et al. 2009), there were no structures of any eukaryotic counterpart. The DHO domain of human CAD was the first eukaryotic DHO for which the crystal structure was solved (Grande-Garcia et al. 2014; Lallous et al. 2012). In agreement with studies reporting that the proteolytic fragment of CAD retaining DHO activity forms dimers (Davidson et al. 1981), the isolated human DHO domain was shown to be a homodimer in solution (Fig. 17.8a, b) (Lallous et al. 2012). The overall subunit fold is similar to bacterial counterparts, and is also shared with a large number of enzymes –most of which catalyze the hydrolysis of substrates at amide or ester groups– forming the amidohydrolase superfamily of proteins (Holm and Sander 1997). Each subunit is structured in a "TIM" barrel with eight strands of parallel β-sheet flanked on the outer surface by α-helices, and a smaller adjacent β-stranded subdomain composed of the N- and C-terminal regions of the protein (Fig. 17.8c). This adjacent subdomain is continued by a C-terminal extension that stretches through the bottom of the barrel, and places the N- and C-ends on opposite sides of the globular domain, a convenient arrangement for the intercalation of DHO in the middle of CAD.

As in other members of the amidohydrolase superfamily, the active center of the DHO domain of CAD locates on the C-terminal edge of the β-barrel, a cavity shaped by the loops connecting the β-strands with the outer α-helices (Fig. 17.8c). There are two Zn^{2+} ions (Zn-α and Zn-β) coordinated by four His and one Asp at conserved positions in the active site (Fig. 17.8d). The metals are bridged by the side chain of a carboxylated Lys and by a water molecule that is activated by the metal ions for nucleophilic attack (Porter et al. 2004). Human DHO has a third Zn^{2+} ion (Zn-γ) approximately at the center of the β-barrel, which is not found in bacterial DHOs or in other members of the amidohydrolase superfamily (Fig. 17.8c, d). This Zn-γ interacts with Zn-α through the side chain of a rare histidine (H1471) with negative charge (called histidinate anion). Although Zn-γ appears to be too far to participate directly in catalysis, mutations that impede the binding of this metal are shown to reduce the activity of the protein to half (Grande-Garcia et al. 2014). Interestingly, the introduction by site-directed mutagenesis of the third Zn^{2+} into a bacterial DHO, increased the activity and stability of the protein (Huang and Huang 2015). These results suggest that Zn-γ could play a

role in the stabilization of the DHO domain of CAD, and perhaps influence the electrostatic environment at the active site (Grande-Garcia et al. 2014).

Despite having a low sequence identity (15%), the human and *E. coli* DHOs active sites are virtually identical and both enzymes are proposed to share a common catalytic mechanism (Grande-Garcia et al. 2014; Porter et al. 2004). The conversion of carbamoyl aspartate to dihydroorotate is reversible and pH-dependent, with the forward and reverse reactions reaching equilibrium at approximately neutral pH (Christopherson and Jones 1980). In the synthesis of dihydroorotate, favored at low pH, the water molecule bridging Zn-α and Zn-β is displaced by the binding of the side chain of carbamoyl aspartate (Fig. 17.8d). The metals neutralize the negative charge of the carboxylate group, increasing its susceptibility to a nucleophilic attack by the amino group of carbamoyl aspartate. To favor the reaction, the amino group is deprotonated by an Asp (D1686 in human DHO) acting as the general base. The reaction proceeds by formation of a tetrahedral intermediate that becomes stabilized by the metal ions. Then, the OH leaving group is protonated, collapsing the transition state and releasing dihydroorotate and a water molecule that is retained between the two metal ions. In turn, the hydrolysis of dihydroorotate is favored above pH 8 and involves the nucleophilic attack of the bridging water (or hydroxide ion) to the amide bond of dihydroorotate (Fig. 17.8d). This reaction, rather than the forward synthesis of dihydroorotate, is favored under physiological conditions (Christopherson and Jones 1980). It is proposed that the equilibrium of the reactions could be displaced toward the synthesis of dihydroorotate by the location of CAD near the mitochondria, which may facilitate the efficient capture of dihydroorotate by DHODH, the enzyme catalyzing the next step in de novo pathway (Evans and Guy 2004) (Fig. 17.1).

The DHO subunit is rigidly built by tight hydrophobic packing of the central β-barrel and the α-helical palisade. Indeed, different crystal structures of human and *E. coli* DHOs show no significant conformational changes upon binding of substrates or different inhibitors at the active site. There is only one exception, a flexible loop that adopts an open solvent-exposed position or a closed conformation whether dihydroorotate or carbamoyl aspartate are bound, respectively, to the active site (del Cano-Ochoa et al. 2018; Grande-Garcia et al. 2014; Lee et al. 2005) (Fig. 17.8c, d). This loop plays an important catalytic role, placing the substrate in correct orientation, stabilizing the transition state of the reaction and excluding the solvent molecules from the active site.

The position of the flexible loops near the dimerization interface of human DHO suggests a possible coordination between both active sites (Fig. 17.8b). However, enzymatic assays have failed to detect signs of cooperativity in human DHO (del Cano-Ochoa et al. 2018; Grande-Garcia et al. 2014). In contrast, in *E. coli* DHO, the subunits dimerize through the loops above the β-barrel, rather than by lateral contacts as in human DHO, and the movements of the flexible loop appear related to the cooperativity effect observed between the two confronted active sites (Lee et al. 2005) (Fig. 17.2b). In the *A. aeolicus* DHO/ATC complex, on the other hand,

the DHO subunits make lateral contacts but the subunits are rotated 180º compared to human DHO (Fig. 17.2c). As a result, adjacent DHO subunits direct their active sites towards different ATC trimers. Interestingly, *A. aeolicus* DHO lacks a catalytic flexible loop and requires the interaction with a loop from ATC to complete the active site and achieve maximal activity (Prange et al. 2019; Zhang et al. 2009). It is intriguing how some DHOs equipped with a flexible loop are catalytically independent, whereas others have an unfinished active site that needs to be complemented by a stable association with ATC. Then, we wonder why the DHO domain of CAD, which has a catalytic flexible loop, is covalently engaged to an ATC domain that is not necessary for its activity. The answer to this question is that probably the linkage of both domains is not intended to increase the efficacy of DHO and must fulfill other purposes. Indeed, the recent crystal structure of the inactive DHO-like domain from the CAD-like protein of the fungus *Chaetomium thermophilum* (Fig. 17.8e) proved that as predicted (Souciet et al. 1989), the catalytic residues and Zn^{2+} ions are missing from the active site (Moreno-Morcillo et al. 2017). However, this inactive domain forms homodimers in an identical quaternary arrangement as human DHO (Fig. 17.8f). The preservation of the dimer architecture strongly suggests that the DHO domain plays a conserved structural role within the context of the full-length protein oligomerization. The linkage with ATC must harness both domains for the assembly of a multienzymatic protein machinery that appears conserved both in animals and fungi (Moreno-Morcillo et al. 2017).

Putting the Pieces Together for the Pyrimidine Factory

Based on the expected similarity of the GLN and SYN domains of CAD with *E. coli* CPS and human CPS-1 and on the crystal structures of the human DHO and ATC structures, we can build a hypothetical model of the full-length protein with the four domains arranged as beads on a string (Fig. 17.9a). However, this model is utterly useless unless we define how this protein self-assembles into larger particles that explain the communication and coordination between the different activities.

Early studies reported that CAD self-assembles into a mixture of oligomers (Coleman et al. 1977), mostly hexamers of ~1.5 MDa in size (Lee et al. 1985). Since the proteolytic fragments retaining DHO and ATC activities were found to form dimers and trimers, respectively (Davidson et al. 1981; Hemmens and Carrey 1994; Kelly et al. 1986), an idea prevailed, that the CAD hexamers could result from the association of three proteins through their respective ATC domains, and that two of these trimers could further dimerize through their DHO domains (Carrey 1995b; Evans 1986). A similar organization was proposed for the architecture of the CAD-like protein in *Neurospora* (Makoff et al. 1978), although in this model the dimerization of the trimers was proposed to be mediated by the CPS region.

The key role of ATC in the molecular organization of CAD was demonstrated by Qiu and Davidson, who proved that mutations in the predicted ATC trimer interface

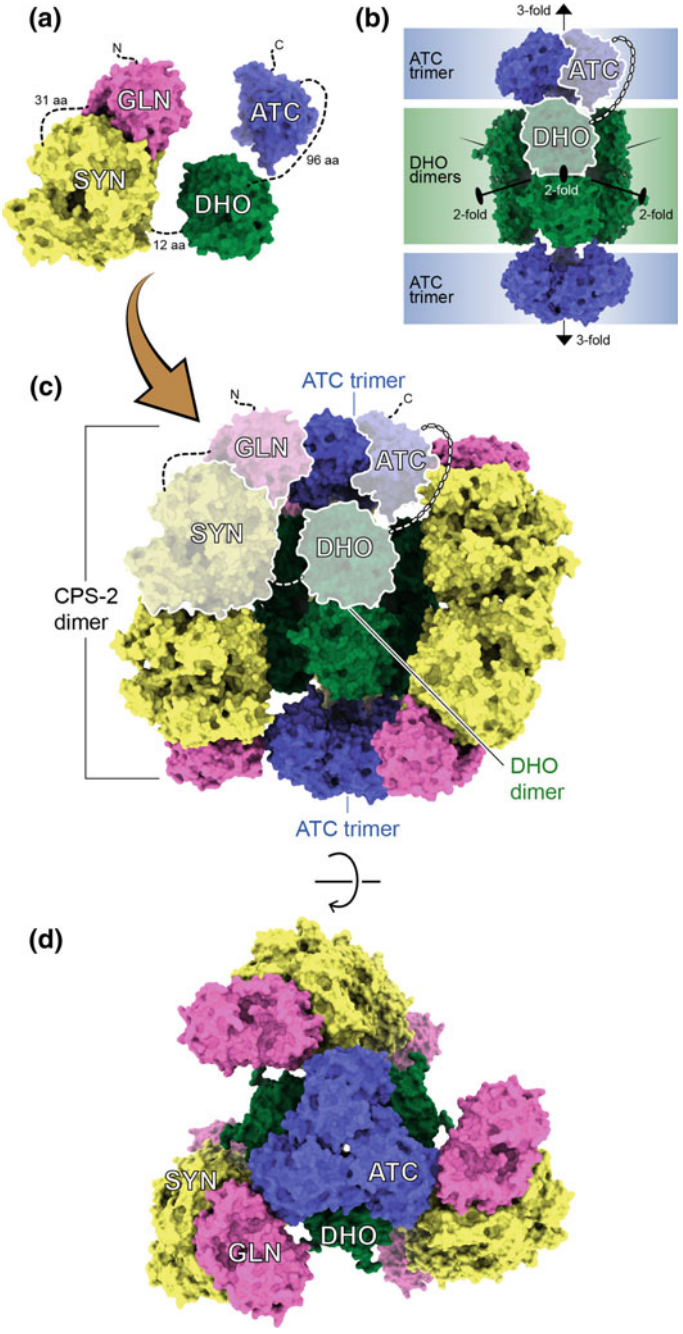
(a)
N
C
31 aa
GLN
ATC
SYN
DHO
96 aa
12 aa
(b)
3-fold
ATC trimer
ATC
DHO
DHO dimers
2-fold
2-fold
2-fold
ATC trimer
3-fold
(c)
ATC trimer
N
C
GLN
ATC
SYN
DHO
CPS-2 dimer
DHO dimer
ATC trimer
(d)
SYN
ATC
GLN
DHO

◂**Fig. 17.9** Model of the architecture of CAD. **a** Model of CAD full-length protein with the GLN, SYN, DHO and ATC domains as beads on a string. Dashed lines indicate linker regions of different lengths. **b** Model of the bi-functional DHO-ATC construct forming an hexamer (or "dimer of trimers"). **c**, **d** Hypothetical model of CAD hexameric particle in two perpendicular orientations

caused the dissociation of CAD hexamers (Qiu and Davidson 1998, 2000). However, this study ruled out the possibility that the DHO or CPS domains participated directly in the oligomerization of the particle.

To challenge the idea proposed by Carrey that CAD could assemble as a "dimer of trimers" (Carrey 1995b), our group made a construct spanning the DHO and ATC domains of human CAD, including the long linker in between. This bi-functional construct was shown to form stable homo-hexamers in solution, and point mutations in the ATC or DHO oligomerization interfaces resulted in the formation of dimers and trimers, respectively (Moreno-Morcillo et al. 2017). These results indicate that CAD indeed assembles as a "dimer of trimers" and suggest that the DHO and ATC domains provide a central scaffold for the architecture of the particle (Fig. 17.9b). Moreover, we proved that despite having an inactive DHO-like domain, a similar construct from the CAD-like protein from *C. thermophilum* behaves in the same manner, supporting that CAD and CAD-like particles share a common architecture (Moreno-Morcillo et al. 2017).

Taking into consideration previous models (Carrey 1995b; Evans 1986; Makoff et al. 1978) and gathering all the current structural information, we propose a plausible blueprint for the architecture of CAD (Fig. 17.9c, d). The DHO and ATC domains form the central axis of the particle. The ATC monomers are arranged into two trimers occupying apical positions and with the active sites face-to-face. Three DHO dimers interpose in between the ATC trimers, with their long axes in parallel to the threefold axis of the ATC domains and with the active sites facing inwards. This results in a closed hexameric structure of 190 × 100 Å, with D3 symmetry (a threefold axis with three perpendicular twofold axes) and a delimited inner space of ∼120 × 50 Å (Moreno-Morcillo et al. 2017; Moreno-Morcillo and Ramon-Maiques 2017). This disposition of the ATC and DHO domains is somehow reminiscent of the noncovalent association between the regulatory and catalytic subunits of *E. coli* ATC or between the ATC and DHO enzymes of *A. aeolicus* (Fig. 17.2b, c).

Negative staining electron microscopy data indicated that the hexamer formed by the DHO-ATC construct is quite flexible (Moreno-Morcillo et al. 2017). The long sequence connecting the DHO and ATC domains likely restrains the relative position of both domains, but allows certain flexibility between them. Perhaps the DHO dimers could tilt around their twofold axes, allowing the separation or approximation of the ATC trimers, into tighter or more relaxed states that limit the conformational changes required for catalysis, in a similar manner to the allosteric transitions described in the *E. coli* ATC holoenzyme (Fig. 17.2b) (Lipscomb 1994; Lipscomb and Kantrowitz 2011; Ruiz-Ramos et al. 2016).

Some regions of the long linker connecting DHO and ATC could make interactions with both domains, and also perhaps with the GLN/SYN domains, adding stability to the assembly. However, a part of the linker must be exposed to the solvent to explain the high sensitivity to proteases and also, for being phosphorylated. Two different studies reported that residue S1859 at the linker sequence in human CAD is phosphorylated by S6 kinase in the downstream of mTORC1 pathway, and that this modification increases the rate of de novo pyrimidine synthesis (Ben-Sahra et al. 2013; Robitaille et al. 2013). Interestingly, the phosphorylation also favors the oligomerization of CAD (Robitaille et al. 2013), in agreement with a possible role of the linker in the stabilization of the particle.

To complete the model, six CPS-2, formed by the GLN and SYN domains, need to be added to the central DHO-ATC framework. It is clear by similarity to other CPSs and by biochemical data that the GLN and SYN domains will form a tight heterodimer. Also, the observation that proteolytic fragments of *Neurospora* CAD-like protein with CPS activity form dimers (Makoff et al. 1978), suggests that CPS-2 could further dimerize through the allosteric regions, similarly to the dimers observed in the crystal structures of *E. coli* CPS and human CPS-1 (Figs. 17.3c and 17.4b). We propose that the six CPS-2 could be organized as three dimers surrounding the central DHO-ATC assembly, with the twofold axes in the equatorial plane of this globular complex of $\sim 200 \times 200$ Å (Fig. 17.9c, d).

Despite the symmetrical beauty, this model could be wrong and needs more structural data to be validated. A detailed characterization of the particle, probably by using high resolution cryo-microscopy, will shed light on the evolutionary advantages of a single multienzymatic protein versus the mono-functional homologs in prokaryotes. Till then, it can only be hypothesized that the engineering of several enzymatic activities into a single polypeptide likely improves the metabolic efficiency in a number of ways (Davidson et al. 1993; Stark 1977). Firstly, similar to a bacterial operon, the fusion of the enzymes into a single polypeptide ensures the coordinated and stoichiometric production of the enzymatic activities. In addition, the covalent linkage favors the co-localization of the different activities within the cell. The proximity between domains might also enhance the specificity for their association, and this could also result in increased stability compared to the isolated proteins. Another advantage for the formation of a complex such as the one proposed in Fig. 17.9, is the close proximity between active sites, which should favor the transfer or "channeling" of intermediate metabolites. The concept of channeling was introduced by Davis to explain the existence of two different pools of CP in the cell for the de novo biosynthesis of pyrimidines and arginine (Davis 1972). The fact that in de novo pyrimidine synthesis there is no significant accumulation of any of the intermediates between bicarbonate and UMP, led M. E. Jones to consider that the enzymes could have a special structural conformation that ensures products and substrates to reach their destination (Jones 1971, 1980; Shoaf and Jones 1971). The proposed model accounts for the partial channeling of CP reported by different studies in mammalian CAD and in the CAD-like from yeast (Christopherson and Jones 1980; Mally et al. 1980; Otsuki et al. 1982; Penverne et al. 1994). Channeling starts at the GLN domain following the ~ 90 Å

tunnel running through the interior of the SYN domain. The orientation of the CPS-2 dimers in the particle would be such that the exit of this intramolecular tunnel could face the gaps between the DHO dimers. In this manner, the CP would be delivered from the SYN domains directly into the central cavity of the particle where it would diffuse a short distance to reach the ATC active site without exposure to the bulk solvent.

This large multi-subunit and multi-domain assembly might also allow for a more complex mechanism of control. It is possible that binding of the allosteric effectors, UTP and PRPP, at the regulatory domains could induce conformational changes as those observed in CPS-1 upon acetylglutamate binding (de Cima et al. 2015). Changes in the relative orientation of the CPS-2 dimer could be transmitted to the rest of the protein, inducing the rotation and translation of the DHO dimers and ATC trimers along their respective symmetry axes, and reversely, conformational changes in the ATC trimer due to substrate or PALA binding, could be communicated to the outer CPS-2 dimers. This conformational cross-talk would explain the mutual effects between both enzymatic activities that E. Carrey described as "reciprocal allostery" (Irvine et al. 1997). The concerted movements of the domains could modulate the affinity for the substrates, the rate and the coupling of the reactions, the channeling of intermediates as well as the flux of substrates and products in and out the particle. In a stretch of imagination, one can envision that the hexameric particle could transit through a series of conformational states with different overall activity, and that a number of external inputs such as allosteric effectors, phosphorylations and other posttranslational modifications or interactions with other cellular components could displace the conformational equilibrium, thus contributing to the regulation of the de novo pyrimidine pathway.

CAD in Human Diseases

Whereas a complete lack of activity in any of the enzymatic activities for de novo biosynthesis of pyrimidines appears to be incompatible with life, mutations causing impairment of the activities associate with different human disorders. Defects in DHODH activity are associated with Miller syndrome, a malformation disorder with no intellectual damage (Ng et al. 2010). Also, UMPS malfunctions cause orotic aciduria, a condition in which the accumulation of orotate produces intellectual and motor impairment, seizures and immunodeficiency (Imaeda et al. 1998; Loffler et al. 2015). However, until recently, no human disease had been related to a partial loss of CAD activity. Mutations compromising CAD function were known to cause severe malformations and death in model organisms such as *Drosophila* (rudimentary phenotype) (Norby 1970), zebrafish (perplexed phenotype) (Willer et al. 2005) and *C. elegans* (Franks et al. 2006). These results led to the assumption that a reduced function of CAD would be lethal and explained that no human diseases were associated with failures in this protein.

However, in 2015, H. Freeze and colleagues described the first case of a 4-year old boy with a severe impairment of protein glycosylation caused by a partial deficit in CAD (Ng et al. 2015). The identified mutation, R2024Q, maps in the active site of ATC, and it was shown to severely reduce the activity of the isolated ATC domain and its affinity for the substrates (Ruiz-Ramos et al. 2016). One year later, a second study reported three families with young children carrying mutations in CAD that caused developmental delay, epileptic encephalopathy, anemia and seizures (Koch et al. 2017). While the untreated disease course is lethal in early childhood, both studies reported that patients survived upon an oral treatment with uridine, which compensates by salvage the defects of the de novo pyrimidine synthesis. Since then, new cases of children with potential CAD-deficits have continued appearing (H. Freeze personal communication).

The identification of CAD-deficiency as a treatable metabolic disorder stresses the importance of an early detection in newborns and young children (Koch et al. 2017). However, the diagnosis is difficult (e.g. numerous symptoms, pyrimidine levels in urine might seem normal) and so far, patients were only diagnosed after complete exome sequencing (Koch et al. 2017; Ng et al. 2015). As these sequencing techniques become more affordable, a major challenge that remains, giving our fragmented knowledge about CAD, is the distinction between disease-causing mutations and simple protein polymorphisms. Thus, deciphering the architecture of CAD is not only key to unveil the catalytic and regulatory mechanisms of a central metabolic machinery and to guide in the design of specific inhibitors with a potential chemotherapeutic use, but also is of paramount importance for helping in the correct diagnosis and treatment of patients.

References

Allewell NM (1989) *Escherichia coli* aspartate transcarbamoylase: structure, energetics, and catalytic and regulatory mechanisms. Annu Rev Biophys Biophys Chem 18:71–92

Anderson PM (1986) Carbamoyl-phosphate synthetase: an example of effects on enzyme properties of shifting an equilibrium between active monomer and active oligomer. Biochemistry 25(19):5576–5582

Anderson PM, Meister A (1965) Evidence for an activated form of carbon dioxide in the reaction catalyzed by *Escherichia coli* carbamyl phosphate synthetase. Biochemistry 4(12):2803–2809

Anderson PM, Meister A (1966) Bicarbonate-dependent cleavage of adenosine triphosphate and other reactions catalyzed by *Escherichia coli* carbamyl phosphate synthetase. Biochemistry 5 (10):3157–3163

Antonelli R, Estevez L, Denis-Duphil M (1998) Carbamyl-phosphate synthetase domain of the yeast multifunctional protein Ura2 is necessary for aspartate transcarbamylase inhibition by UTP. FEBS Lett 422(2):170–174

Ben-Sahra I, Howell JJ, Asara JM et al (2013) Stimulation of de novo pyrimidine synthesis by growth signaling through mTOR and S6K1. Science 339(6125):1323–1328

Braxton BL, Mullins LS, Raushel FM et al (1992) Quantifying the allosteric properties of *Escherichia coli* carbamyl phosphate synthetase: determination of thermodynamic linked-function parameters in an ordered kinetic mechanism. Biochemistry 31(8):2309–2316

Braxton BL, Mullins LS, Raushel FM et al (1996) Allosteric effects of carbamoyl phosphate synthetase from *Escherichia coli* are entropy-driven. Biochemistry 35(36):11918–11924

Britton HG, Rubio V, Grisolia S (1979) Mechanism of carbamoyl-phosphate synthetase. Properties of the two binding sites for ATP. Eur J Biochem 102(2):521–530

Brown EG (1998) Pyrimdines, ring nitrogen and key biomolecules: the biochemistry of N-heterocycles. Springer

Bueso J, Cervera J, Fresquet V et al (1999) Photoaffinity labeling with the activator IMP and site-directed mutagenesis of histidine 995 of carbamoyl phosphate synthetase from *Escherichia coli* demonstrate that the binding site for IMP overlaps with that for the inhibitor UMP. Biochemistry 38(13):3910–3917

Carrey EA (1995a) Key enzymes in the biosynthesis of purines and pyrimidines: their regulation by allosteric effectors and by phosphorylation. Biochem Soc Trans 23(4):899–902

Carrey EA (1995b) The shape of CAD J. N. Davidson Paths to pyrimidines - an international newsletter

Carrey EA, Hardie DG (1988) Mapping of catalytic domains and phosphorylation sites in the multifunctional pyrimidine-biosynthetic protein CAD. Eur J Biochem 171(3):583–588

Carrey EA, Campbell DG, Hardie DG (1985) Phosphorylation and activation of hamster carbamyl phosphate synthetase II by cAMP-dependent protein kinase. A novel mechanism for regulation of pyrimidine nucleotide biosynthesis. EMBO J 4(13B):3735–3742

Cervera J, Conejero-Lara F, Ruiz-Sanz J et al (1993) The influence of effectors and subunit interactions on *Escherichia coli* carbamoyl-phosphate synthetase studied by differential scanning calorimetry. J Biol Chem 268(17):12504–12511

Cervera J, Bendala E, Britton HG et al (1996) Photoaffinity labeling with UMP of lysine 992 of carbamyl phosphate synthetase from *Escherichia coli* allows identification of the binding site for the pyrimidine inhibitor. Biochemistry 35(22):7247–7255

Chaparian MG, Evans DR (1991) The catalytic mechanism of the amidotransferase domain of the Syrian hamster multifunctional protein CAD. Evidence for a CAD-glutamyl covalent intermediate in the formation of carbamyl phosphate. J Biol Chem 266(6):3387–3395

Christopherson RI, Jones ME (1980) The overall synthesis of L-5,6-dihydroorotate by multienzymatic protein pyr1-3 from hamster cells. Kinetic studies, substrate channeling, and the effects of inhibitors. J Biol Chem 255(23):11381–11395

Coleman PF, Suttle DP, Stark GR (1977) Purification from hamster cells of the multifunctional protein that initiates de novo synthesis of pyrimidine nucleotides. J Biol Chem 252(18):6379–6385

Collins KD, Stark GR (1969) Aspartate transcarbamylase. Studies of the catalytic subunit by ultraviolet difference spectroscopy. J Biol Chem 244(7):1869–1877

Collins KD, Stark GR (1971) Aspartate transcarbamylase interaction with the transition state analogue N-(phosphonacetyl)-L-aspartate. J Biol Chem 246(21):6599–6605

Czerwinski RM, Mareya SM, Raushel FM (1995) Regulatory changes in the control of carbamoyl phosphate synthetase induced by truncation and mutagenesis of the allosteric binding domain. Biochemistry 34(42):13920–13927

Davidson JN, Patterson D (1979) Alteration in structure of multifunctional protein from Chinese hamster ovary cells defective in pyrimidine biosynthesis. Proc Natl Acad Sci U S A 76 (4):1731–1735

Davidson JN, Rumsby PC, Tamaren J (1981) Organization of a multifunctional protein in pyrimidine biosynthesis. Analyses of active, tryptic fragments. J Biol Chem 256(10):5220–5225

Davidson JN, Rao GN, Niswander L et al (1990) Organization and nucleotide sequence of the 3′ end of the human CAD gene. DNA Cell Biol 9(9):667–676

Davidson JN, Chen KC, Jamison RS et al (1993) The evolutionary history of the first three enzymes in pyrimidine biosynthesis. BioEssays 15(3):157–164

Davis RH (1972) Metabolite distribution in cells. Science 178(4063):835–840

de Cima S, Polo LM, Diez-Fernandez C et al (2015) Structure of human carbamoyl phosphate synthetase: deciphering the on/off switch of human ureagenesis. Sci Rep 5:16950

del Cano-Ochoa F, Grande-Garcia A, Reverte-Lopez M et al (2018) Characterization of the catalytic flexible loop in the dihydroorotase domain of the human multi-enzymatic protein CAD. J Biol Chem 293(49):18903–18913

Denis-Duphil M (1989) Pyrimidine biosynthesis in *Saccharomyces cerevisiae*: the ura2 cluster gene, its multifunctional enzyme product, and other structural or regulatory genes involved in de novo UMP synthesis. Biochem Cell Biol 67(9):612–631

Denis-Duphil M, Lecaer JP, Hardie DG et al (1990) Yeast carbamoyl-phosphate-synthetase–aspartate-transcarbamylase multidomain protein is phosphorylated in vitro by cAMP-dependent protein kinase. Eur J Biochem 193(2):581–587

Diez-Fernandez C, Martinez AI, Pekkala S et al (2013) Molecular characterization of carbamoyl-phosphate synthetase (CPS1) deficiency using human recombinant CPS1 as a key tool. Hum Mutat 34(8):1149–1159

Eroglu B, Powers-Lee SG (2002) Unmasking a functional allosteric domain in an allosterically nonresponsive carbamoyl-phosphate synthetase. J Biol Chem 277(47):45466–45472

Evans DR (1986) CAD, a chimeric protein that initiates de novo pyrimidine biosynthesis in higher eukaryotes. In: Coggings JR, Hardie DG (eds) Multidomain proteins—structure and evolution. Elsevier

Evans DR, Guy HI (2004) Mammalian pyrimidine biosynthesis: fresh insights into an ancient pathway. J Biol Chem 279(32):33035–33038

Faure M, Camonis JH, Jacquet M (1989) Molecular characterization of a *Dictyostelium discoideum* gene encoding a multifunctional enzyme of the pyrimidine pathway. Eur J Biochem 179(2):345–358

Fawaz MV, Topper ME, Firestine SM (2011) The ATP-grasp enzymes. Bioorg Chem 39(5–6):185–191

Fields C, Brichta D, Shepherdson M et al (1999) Phylogenetic analysis and classification of dihydroorotases: a complex history for a complex enzyme. Paths Pyrimidines 7:49–63

Franks DM, Izumikawa T, Kitagawa H et al (2006) *C. elegans* pharyngeal morphogenesis requires both de novo synthesis of pyrimidines and synthesis of heparan sulfate proteoglycans. Dev Biol 296(2):409–420

Freund JN, Jarry BP (1987) The rudimentary gene of *Drosophila melanogaster* encodes four enzymic functions. J Mol Biol 193(1):1–13

Gaertner FH (1978) Unique catalytic properties of enzyme clusters. Trends Biochem Sci 3:63–65

Gerhart JC, Holoubek H (1967) The purification of aspartate transcarbamylase of *Escherichia coli* and separation of its protein subunits. J Biol Chem 242(12):2886–2892

Gouaux JE, Krause KL, Lipscomb WN (1987) The catalytic mechanism of *Escherichia coli* aspartate carbamoyltransferase: a molecular modelling study. Biochem Biophys Res Commun 142(3):893–897

Grande-Garcia A, Lallous N, Diaz-Tejada C et al (2014) Structure, functional characterization, and evolution of the dihydroorotase domain of human CAD. Structure 22(2):185–198

Graves LM, Guy HI, Kozlowski P et al (2000) Regulation of carbamoyl phosphate synthetase by MAP kinase. Nature 403(6767):328–332

Guy HI, Evans DR (1994) Cloning, expression, and functional interactions of the amidotransferase domain of mammalian CAD carbamyl phosphate synthetase. J Biol Chem 269(10):7702–7708

Hemmens B, Carrey EA (1994) Proteolytic cleavage of the multienzyme polypeptide CAD to release the mammalian aspartate transcarbamoylase. Biochemical comparison with the homologous *Escherichia coli* catalytic subunit. Eur J Biochem 225(3):845–853

Hewagama A, Guy HI, Vickrey JF et al (1999) Functional linkage between the glutaminase and synthetase domains of carbamoyl-phosphate synthetase. Role of serine 44 in carbamoyl-phosphate synthetase-aspartate carbamoyltransferase-dihydroorotase (cad). J Biol Chem 274(40):28240–28245

Holden HM, Thoden JB, Raushel FM (1998) Carbamoyl phosphate synthetase: a tunnel runs through it. Curr Opin Struct Biol 8(6):679–685

Holm L, Sander C (1997) An evolutionary treasure: unification of a broad set of amidohydrolases related to urease. Proteins 28(1):72–82

Hoogenraad NJ, Levine RL, Kretchmer N (1971) Copurification of carbamoyl phosphate synthetase and aspartate transcarbamoylase from mouse spleen. Biochem Biophys Res Commun 44(4):981–988

Huang YH, Huang CY (2015) Creation of a putative third metal binding site in type II dihydroorotases significantly enhances enzyme activity. Protein Pept Lett 22(12):1117–1122

Imaeda M, Sumi S, Imaeda H et al (1998) Hereditary orotic aciduria heterozygotes accompanied with neurological symptoms. Tohoku J Exp Med 185(1):67–70

Irvine HS, Shaw SM, Paton A et al (1997) A reciprocal allosteric mechanism for efficient transfer of labile intermediates between active sites in CAD, the mammalian pyrimidine-biosynthetic multienzyme polypeptide. Eur J Biochem 247(3):1063–1073

Jacobson GR, Stark GR (1973) Aspartate transcarbamylases. In: Boyer PD (ed) The enzymes. Academic Press (Elsevier)

Jones ME (1971) Regulation of pyrimidine and arginine biosynthesis in mammals. Adv Enzyme Regul 9:19–49

Jones ME (1980) Pyrimidine nucleotide biosynthesis in animals: genes, enzymes, and regulation of UMP biosynthesis. Annu Rev Biochem 49(1):253–279

Kelly RE, Mally MI, Evans DR (1986) The dihydroorotase domain of the multifunctional protein CAD. Subunit structure, zinc content, and kinetics. J Biol Chem 261(13):6073–6083

Kempe TD, Swyryd EA, Bruist M et al (1976) Stable mutants of mammalian cells that overproduce the first three enzymes of pyrimidine nucleotide biosynthesis. Cell 9(4 Pt 1):541–550

Kim H, Kelly RE, Evans DR (1992) The structural organization of the hamster multifunctional protein CAD. Controlled proteolysis, domains, and linkers. J Biol Chem 267(10):7177–7184

Koch J, Mayr JA, Alhaddad B et al (2017) CAD mutations and uridine-responsive epileptic encephalopathy. Brain 140(Pt 2):279–286

Lacroute F, Pierard A, Grenson M et al (1965) The biosynthesis of carbamoyl phosphate in *Saccharomyces cerevisiae*. J Gen Microbiol 40(1):127–142

Lallous N, Grande-Garcia A, Molina R et al (2012) Expression, purification, crystallization and preliminary X-ray diffraction analysis of the dihydroorotase domain of human CAD. Acta Crystallogr, Sect F: Struct Biol Cryst Commun 68(Pt 11):1341–1345

Lee L, Kelly RE, Pastra-Landis SC et al (1985) Oligomeric structure of the multifunctional protein CAD that initiates pyrimidine biosynthesis in mammalian cells. Proc Natl Acad Sci U S A 82 (20):6802–6806

Lee M, Chan CW, Mitchell Guss J et al (2005) Dihydroorotase from *Escherichia coli*: loop movement and cooperativity between subunits. J Mol Biol 348(3):523–533

LiCata VJ, Allewell NM (1997) Is substrate inhibition a consequence of allostery in aspartate transcarbamylase? Biophys Chem 64(1–3):225–234

Lipscomb WN (1994) Aspartate transcarbamylase from *Escherichia coli*: activity and regulation. Adv Enzymol Relat Areas Mol Biol 68:67–151

Lipscomb WN, Kantrowitz ER (2011) Structure and mechanisms of *Escherichia coli* aspartate transcarbamoylase. Acc Chem Res 45(3):444–453

Liu X, Guy HI, Evans DR (1994) Identification of the regulatory domain of the mammalian multifunctional protein CAD by the construction of an *Escherichia coli* hamster hybrid carbamyl-phosphate synthetase. J Biol Chem 269(44):27747–27755

Loffler M, Carrey EA, Zameitat E (2015) Orotic acid, more than just an intermediate of pyrimidine de novo synthesis. J Genet Genomics 42(5):207–219

Lue PF, Kaplan JG (1969) The aspartate transcarbamylase and carbamoyl phosphate synthetase of yeast: a multi-functional enzyme complex. Biochem Biophys Res Commun 34(4):426–433

Lusty CJ (1981) Catalytically active monomer and dimer forms of rat liver carbamoyl-phosphate synthetase. Biochemistry 20(13):3665–3674

Makoff AJ, Buxton FP, Radford A (1978) A possible model for the structure of the Neurospora carbamoyl phosphate synthase-aspartate carbamoyl transferase complex enzyme. Mol Gen Genet 161(3):297–304

Mally MI, Grayson DR, Evans DR (1980) Catalytic synergy in the multifunctional protein that initiates pyrimidine biosynthesis in Syrian hamster cells. J Biol Chem 255(23):11372–11380
Mally MI, Grayson DR, Evans DR (1981) Controlled proteolysis of the multifunctional protein that initiates pyrimidine biosynthesis in mammalian cells: evidence for discrete structural domains. Proc Natl Acad Sci U S A 78(11):6647–6651
Meister A (1989) Mechanism and regulation of the glutamine-dependent carbamyl phosphate synthetase of *Escherichia coli*. Adv Enzymol Relat Areas Mol Biol 62:315–374
Miles BW, Raushel FM (2000) Synchronization of the three reaction centers within carbamoyl phosphate synthetase. Biochemistry 39(17):5051–5056
Miles BW, Banzon JA, Raushel FM (1998) Regulatory control of the amidotransferase domain of carbamoyl phosphate synthetase. Biochemistry 37(47):16773–16779
Miran SG, Chang SH, Raushel FM (1991) Role of the four conserved histidine residues in the amidotransferase domain of carbamoyl phosphate synthetase. Biochemistry 30(32):7901–7907
Mora P, Rubio V, Fresquet V et al (1999) Localization of the site for the nucleotide effectors of *Escherichia coli* carbamoyl phosphate synthetase using site-directed mutagenesis. FEBS Lett 446(1):133–136
Moreno-Morcillo M, Ramon-Maiques S (2017) CAD: a multifunctionl protein leading de novo pyrimidine biosynthesis. In: Encyclopedia of life sciences. John Wiley and Sons
Moreno-Morcillo M, Grande-Garcia A, Ruiz-Ramos A et al (2017) Structural Insight into the Core of CAD, the multifunctional protein leading de novo pyrimidine biosynthesis. Structure 25 (6):912–923 e915
Mori M, Tatibana M (1978) A multienzyme complex of carbamoyl-phosphate synthase (glutamine): aspartate carbamoyltransferase: dihydoorotase (rat ascites hepatoma cells and rat liver). Methods Enzymol 51:111–120
Newell JO, Markby DW, Schachman HK (1989) Cooperative binding of the bisubstrate analog N-(phosphonacetyl)-L-aspartate to aspartate transcarbamoylase and the heterotropic effects of ATP and CTP. J Biol Chem 264(5):2476–2481
Ng SB, Buckingham KJ, Lee C et al (2010) Exome sequencing identifies the cause of a mendelian disorder. Nat Genet 42(1):30–35
Ng BG, Wolfe LA, Ichikawa M et al (2015) Biallelic mutations in CAD, impair de novo pyrimidine biosynthesis and decrease glycosylation precursors. Hum Mol Genet 24(11):3050–3057
Norby S (1970) A specific nutritional requirement for pyrimidines in rudimentary mutants of Drosophila melanogaster. Hereditas 66(2):205–214
Nyhan WL (2005) Nucleotide synthesis via salvage pathway. In: Encyclopedia of life sciences. John Wiley and Sons
Nyunoya H, Lusty CJ (1983) The carB gene of *Escherichia coli*: a duplicated gene coding for the large subunit of carbamoyl-phosphate synthetase. Proc Natl Acad Sci U S A 80(15):4629–4633
Nyunoya H, Lusty CJ (1984) Sequence of the small subunit of yeast carbamyl phosphate synthetase and identification of its catalytic domain. J Biol Chem 259(15):9790–9798
Nyunoya H, Broglie KE, Widgren EE et al (1985) Characterization and derivation of the gene coding for mitochondrial carbamyl phosphate synthetase I of rat. J Biol Chem 260(16):9346–9356
Otsuki T, Mori M, Tatibana M (1982) Studies on channeling of carbamoyl-phosphate in the multienzyme complex that initiates pyrimidine biosynthesis in rat ascites hepatoma cells. J Biochem 92(5):1431–1437
Penverne B, Belkaid M, Herve G (1994) In situ behavior of the pyrimidine pathway enzymes in *Saccharomyces cerevisiae*. 4. The channeling of carbamylphosphate to aspartate transcarbamylase and its partition in the pyrimidine and arginine pathways. Arch Biochem Biophys 309(1):85–93
Pierson DL, Brien JM (1980) Human carbamylphosphate synthetase I. Stabilization, purification, and partial characterization of the enzyme from human liver. J Biol Chem 255(16):7891–7895
Porter RW, Modebe MO, Stark GR (1969) Aspartate transcarbamylase. Kinetic studies of the catalytic subunit. J Biol Chem 244(7):1846–1859

Porter TN, Li Y, Raushel FM (2004) Mechanism of the dihydroorotase reaction. Biochemistry 43 (51):16285–16292

Powers-Lee SG, Corina K (1986) Domain structure of rat liver carbamoyl phosphate synthetase I. J Biol Chem 261(33):15349–15352

Prange T, Girard E, Fourme R et al (2019) Pressure-induced activation of latent Dihydroorotase from *Aquifex aeolicus* as revealed by high pressure protein crystallography. FEBS J

Qiu Y, Davidson JN (1998) Aspartate-90 and arginine-269 of hamster aspartate transcarbamylase affect the oligomeric state of a chimaeric protein with an *Escherichia coli* maltose-binding domain. Biochem J 329(Pt 2):243–247

Qiu Y, Davidson JN (2000) Substitutions in the aspartate transcarbamoylase domain of hamster CAD disrupt oligomeric structure. Proc Natl Acad Sci 97(1):97–102

Raushel FM, Thoden JB, Reinhart GD et al (1998) Carbamoyl phosphate synthetase: a crooked path from substrates to products. Curr Opin Chem Biol 2(5):624–632

Robitaille AM, Christen S, Shimobayashi M et al (2013) Quantitative phosphoproteomics reveal mTORC1 activates de novo pyrimidine synthesis. Science 339(6125):1320–1323

Rodriguez-Aparicio LB, Guadalajara AM, Rubio V (1989) Physical location of the site for N-acetyl-L-glutamate, the allosteric activator of carbamoyl phosphate synthetase, in the 20-kilodalton COOH-terminal domain. Biochemistry 28(7):3070–3074

Rubio V (1994) Structure-activity correlations in carbamoyl phosphate synthetases. In: Brändén CI, Schneider G (eds) Carbon dioxide fixation and reduction in biological and model systems. Proceedings of the royal swedish academy of sciences nobel symposium 1991. Oxford University Press

Rubio V, Ramponi G, Grisolia S (1981) Carbamoyl phosphate synthetase I of human liver. Purification, some properties and immunological cross-reactivity with the rat liver enzyme. Biochim Biophys Acta 659(1):150–160

Rubio V, Britton HG, Grisolia S (1983) Mitochondrial carbamoyl phosphate synthetase activity in the absence of N-acetyl-L-glutamate. Mechanism of activation by this cofactor. Eur J Biochem 134(2):337–343

Rubio V, Cervera J, Lusty CJ et al (1991) Domain structure of the large subunit of *Escherichia coli* carbamoyl phosphate synthetase. Location of the binding site for the allosteric inhibitor UMP in the COOH-terminal domain. Biochemistry 30(4):1068–1075

Ruiz-Ramos A, Lallous N, Grande-Garcia A et al (2013) Expression, purification, crystallization and preliminary X-ray diffraction analysis of the aspartate transcarbamoylase domain of human CAD. Acta Crystallogr, Sect F: Struct Biol Cryst Commun 69(Pt 12):1425–1430

Ruiz-Ramos A, Velazquez-Campoy A, Grande-Garcia A et al (2016) Structure and functional characterization of human aspartate transcarbamoylase, the target of the anti-tumoral drug PALA. Structure 24(7):1081–1094

Saeed-Kothe A, Powers-Lee SG (2003) Gain of glutaminase function in mutants of the ammonia-specific frog carbamoyl phosphate synthetase. J Biol Chem 278(29):26722–26726

Schachman HK (1988) Can a simple model account for the allosteric transition of aspartate transcarbamoylase? J Biol Chem 263(35):18583–18586

Schurr MJ, Vickrey JF, Kumar AP et al (1995) Aspartate transcarbamoylase genes of *Pseudomonas putida*: requirement for an inactive dihydroorotase for assembly into the dodecameric holoenzyme. J Bacteriol 177(7):1751–1759

Scully JL, Evans DR (1991) Comparative modeling of mammalian aspartate transcarbamylase. Proteins 9(3):191–206

Shi D, Caldovic L, Tuchman M (2018) Sources and fates of carbamyl phosphate: a labile energy-rich molecule with multiple facets. Biology (Basel) 7(2)

Shigesada K, Stark GR, Maley JA et al (1985) Construction of a cDNA to the hamster CAD gene and its application toward defining the domain for aspartate transcarbamylase. Mol Cell Biol 5 (7):1735–1742

Shoaf WT, Jones ME (1971) Initial steps in pyrimidine synthesis in *Ehrlich ascites* carcinoma. Biochem Biophys Res Commun 45(3):796–802

Simmer JP, Kelly RE, Rinker AG Jr et al (1990) Mammalian carbamyl phosphate synthetase (CPS). DNA sequence and evolution of the CPS domain of the Syrian hamster multifunctional protein CAD. J Biol Chem 265(18):10395–10402

Souciet JL, Nagy M, Le Gouar M et al (1989) Organization of the yeast URA2 gene: identification of a defective dihydroorotase-like domain in the multifunctional carbamoylphosphate synthetase-aspartate transcarbamylase complex. Gene 79(1):59–70

Stark GR (1977) Multifunctional proteins: one gene—more than one enzyme. Trends Biochem Sci 2:64–66

Stevens RC, Reinisch KM, Lipscomb WN (1991) Molecular structure of *Bacillus subtilis* aspartate transcarbamoylase at 3.0 A resolution. Proc Natl Acad Sci U S A 88(14):6087–6091

Swyryd EA, Seaver SS, Stark GR (1974) N-(phosphonacetyl)-L-aspartate, a potent transition state analog inhibitor of aspartate transcarbamylase, blocks proliferation of mammalian cells in culture. J Biol Chem 249(21):6945–6950

Thoden JB, Holden HM, Wesenberg G et al (1997) Structure of carbamoyl phosphate synthetase: a journey of 96 A from substrate to product. Biochemistry 36(21):6305–6316

Thoden JB, Miran SG, Phillips JC et al (1998) Carbamoyl phosphate synthetase: caught in the act of glutamine hydrolysis. Biochemistry 37(25):8825–8831

Thoden JB, Huang X, Raushel FM et al (1999a) The small subunit of carbamoyl phosphate synthetase: snapshots along the reaction pathway. Biochemistry 38(49):16158–16166

Thoden JB, Raushel FM, Benning MM et al (1999b) The structure of carbamoyl phosphate synthetase determined to 2.1 A resolution. Acta Crystallogr D Biol Crystallogr 55(Pt 1):8–24

Thoden JB, Raushel FM, Wesenberg G et al (1999c) The binding of inosine monophosphate to *Escherichia coli* carbamoyl phosphate synthetase. J Biol Chem 274(32):22502–22507

Thoden JB, Wesenberg G, Raushel FM et al (1999d) Carbamoyl phosphate synthetase: closure of the B-domain as a result of nucleotide binding. Biochemistry 38(8):2347–2357

Thoden JB, Phillips GN Jr, Neal TM et al (2001) Molecular structure of dihydroorotase: a paradigm for catalysis through the use of a binuclear metal center. Biochemistry 40(24):6989–6997

Thoden JB, Huang X, Raushel FM et al (2002) Carbamoyl-phosphate synthetase. Creation of an escape route for ammonia. J Biol Chem 277(42):39722–39727

Thoden JB, Huang X, Kim J et al (2004) Long-range allosteric transitions in carbamoyl phosphate synthetase. Protein Sci 13(9):2398–2405

Traut TW, Jones ME (1979) Interconversion of different molecular weight forms of the orotate phosphoribosyltransferase.orotidine-5′-phosphate decarboxylase enzyme complex from mouse Ehrlich ascites cells. J Biol Chem 254(4):1143–1150

Wellner VP, Anderson PM, Meister A (1973) Interaction of *Escherichia coli* carbamyl phosphate synthetase with glutamine. Biochemistry 12(11):2061–2066

Willer GB, Lee VM, Gregg RG et al (2005) Analysis of the Zebrafish perplexed mutation reveals tissue-specific roles for de novo pyrimidine synthesis during development. Genetics 170 (4):1827–1837

Williams LG, Davis RH (1970) Pyrimidine-specific carbamyl phosphate synthetase in *Neurospora crassa*. J Bacteriol 103(2):335–341

Williams LG, Bernhardt S, Davis RH (1970) Copurification of pyrimidine-specific carbamyl phosphate synthetase and aspartate transcarbamylase of *Neurospora crassa*. Biochemistry 9 (22):4329–4335

Yoshida T, Stark GR, Hoogenraad J (1974) Inhibition by N-(phosphonacetyl)-L-aspartate of aspartate transcarbamylase activity and drug-induced cell proliferation in mice. J Biol Chem 249(21):6951–6955

Zhang P, Martin PD, Purcarea C et al (2009) Dihydroorotase from the hyperthermophile *Aquifex aeolicus* is activated by stoichiometric association with aspartate transcarbamoylase and forms a one-pot reactor for pyrimidine biosynthesis. Biochemistry 48(4):766–778

Zrenner R, Stitt M, Sonnewald U et al (2006) Pyrimidine and purine biosynthesis and degradation in plants. Annu Rev Plant Biol 57:805–836